

Politecnico di Torino

Corso di Laurea Magistrale in Ingegneria Chimica e dei Processi

A.a. 2025/2026

Graduation Session Agosto 2026

Numerical Investigation of Phase Change Material (PCM) Melting and Solidification in a Solar Thermal Energy Storage Unit for Rural Applications in Ghana

Supervisor:

prof. Daniele Marchisio

Candidate:

Sandra Adjeiwaa Ameyaw

Acknowledgement

This acknowledgement expresses my sincere gratitude to my academic supervisors, colleagues, and peers for their guidance, encouragement, and support throughout the course of this thesis.

I would like to express my warmest appreciation to Dr. Jude Bonsu from the Kwame Nkrumah University of Science and Technology (KNUST) for his immense support throughout my research. His unwavering commitment to my work and continuous encouragement were invaluable to the successful completion of this thesis. His regular follow-ups and requests for updates on my progress motivated me to remain committed and work even harder.

My sincere appreciation also goes to Prof. Daniele Marchisio and Prof. Olivier Bonnefoy for their valuable advice and guidance even before the commencement of my thesis. I am particularly grateful for the time they took to review my work and provide constructive feedback.

I would also like to express my deepest appreciation to Dr. Daniel Owusu Asante for his guidance and assistance throughout the simulation phase of this research. I encountered several challenges during the simulations, but with his support and guidance, I was able to overcome most of them and make significant progress in my work.

Finally, I would like to express my gratitude to all my peers, particularly Martin Akpalu, whose support and encouragement played an important role in the successful completion of this thesis.

Abstract

In rural areas, post-harvest losses of fruits and vegetables continue to be a major problem, especially where there is no reliable supply of electricity and conventional refrigeration is not available, and so there is little cold storage. Phase change materials (PCMs) provide a promising alternative for passive cooling as they can absorb large amounts of thermal energy as latent heat at relatively stable temperatures. This paper presents a study of the thermal behavior and cooling performance of a PCM based thermal energy storage using computational fluid dynamics (CFD) with the aim to understand the potential application of this system in rural cold storage systems in Ghana.

The enthalpy-porosity method was used to simulate solid-liquid phase change in a transient numerical model developed in ANSYS Fluent. The model considers heat transfer within the PCM and natural convection in the surrounding air. The phase change process is described by the liquid fraction. The numerical method was first validated with the experimental melting data of gallium reported by Gau and Viskanta . The model was able to capture the general experimental melting trend but predicted a higher melting rate at the later stage mainly due to the assumptions of constant thermophysical properties and idealized thermal boundary conditions. The mesh independence study was conducted with mesh size of 1.5 and 1.3 mm and it was found that the predicted temperature and liquid fraction evolution are negligibly different which verifies the adequacy of selected mesh resolution.

The validated model was then used to simulate a 3-D insulated cold-storage enclosure containing five PCM plates. The cooling performance of RT5 PCM was investigated with initial temperature of PCM at 277.5 K and air temperature at 298 K. The findings revealed a rapid drop of air temperature from 298 K to 280 K during the first 100s, followed by a slower rate of cooling as the difference of temperature between air and PCM decreased. At the end of the simulation the air temperature was 279 K and the average PCM temperature increased by a small amount from 277.5 K to 277.6 K. The liquid fraction gradually increased to about 0.20 at 650 s, showing that phase change continued to absorb thermal energy while a large part of the PCM remained solid.

The spatial distribution of liquid fraction also showed the non-uniform melting, with more melting occurring near the air-PCM interface and limited phase change in the interior regions. This behavior shows the effect of the relatively low thermal conductivity of the PCM and hence the thermal resistance to heat penetration. Overall, the results demonstrate the potential of RT5 PCM for passive cooling and decentralized cold storage applications in areas with unreliable electricity supply. However, it is recommended to improve the melting uniformity and cooling performance by enhancing the heat transfer thru improved PCM geometry, metallic fins, conductive additives and optimized PCM arrangement. The results of this work provide a numerical foundation for the development and optimization of PCM-based cold-storage systems for mitigating post-harvest losses in rural Ghana.

Contents

1 Introduction **1**
- 1.1 Background and Motivation . . . 1
- 1.2 Research Objectives . . . 2
  - 1.2.1 Main Objective . . . 2
  - 1.2.2 Specific Objectives . . . 2

2 Literature Review **3**
- 2.1 Cold Storage Systems for Reducing Post-Harvest Losses . . . 3
- 2.2 Phase Change Materials (PCMs) for Thermal Energy Storage . . . 5
  - 2.2.1 Classification of PCMs . . . 5
    - 2.2.1.1 Organic PCMs . . . 5
    - 2.2.1.2 Inorganic PCMs . . . 6
    - 2.2.1.3 Eutectic PCMs . . . 6
  - 2.2.2 Thermophysical Properties of PCMs . . . 6
  - 2.2.3 Principles of Latent Heat Storage . . . 8
- 2.3 CFD Modeling of PCM Systems . . . 9

3 Mathematical Model and Numerical Method **13**
- 3.1 Mathematical Formulation . . . 13
  - 3.1.1 Governing Equations . . . 13
    - 3.1.1.1 Continuity Equation . . . 13
    - 3.1.1.2 Momentum Equation . . . 13
    - 3.1.1.3 Energy Equation . . . 14
  - 3.1.2 Enthalpy-Porosity Method . . . 14
    - 3.1.2.1 Liquid Fraction . . . 14
    - 3.1.2.2 Mushy Zone Modeling . . . 14
- 3.2 Simulation Procedure . . . 14
- 3.3 Geometry and Computational Domain Setup . . . 15
    - 3.3.0.1 2D Geometric Description . . . 15
    - 3.3.0.2 PCM Material Selection and Properties . . . 17
    - 3.3.0.3 Initial Conditions and Domain Initialisation . . . 17
    - 3.3.0.4 3D Geometric Description . . . 18
    - 3.3.0.5 Materials and Methods . . . 18
  - 3.3.1 Mesh Independence Study . . . 19

4 Model Validation **23**
- 4.1 Benchmark Validation . . . 23
  - 4.1.1 Comparison of Melting Interface Positions . . . 24
  - 4.1.2 Validation of Liquid Fraction Prediction . . . 26

5 Results **29**
5.1 Melting Behavior of RT18 PCM . . . 29
5.2 Temperature Distribution During RT18 PCM Melting . . . 32
5.3 3D Cold Storage Melting Behavior . . . 36

6 Discussion **39**
6.1 Thermal Behaviour of PCM During Phase Transition . . . 39
6.2 Cooling Performance of RT5 PCM . . . 39
6.3 Analysis of Melting Distribution and Heat Transfer Mechanisms . . . 40
6.4 Comparison Between RT5 Cooling Performance and PCM Selection Criteria . . . 40
6.5 Implications for Rural Cold Storage Applications in Ghana . . . 41
6.6 Numerical Modelling Considerations and Limitations . . . 41
6.7 Design Optimization Considerations . . . 41
6.7.1 PCM Geometry Optimization . . . 42
6.7.2 Inclusion of Heat Transfer Enhancement Structures . . . 42
6.7.3 PCM Layout Optimization . . . 42
6.7.4 Comparison of PCM Material . . . 42

7 Conclusion and Future Work **43**
7.1 Conclusion . . . 43
7.2 Future Work . . . 44

Index **47**

Bibliographic references **47**

Chapter 1

Introduction

1.1 Background and Motivation

Ghana is a country that borders Togo to the east, Burkina Faso to the north, and Côte d'Ivoire to the west. It is located along the Gulf of Guinea on the coast of West Africa [1][2]. It is one of the geographic regions with the greatest potential for solar energy worldwide, owing to its location near the Equator within the tropical Sun Belt of West Africa. Throughout the year, the country receives abundant solar radiation, with an average irradiance ranging from approximately 4.5 to 6.5 $\mathrm{kWh\,m^{-2}\,day^{-1}}$, depending on the season [3]. This geographical position provides a strong foundation for the deployment of solar energy technologies in the country [4].

Despite this significant solar resource, the country's access to energy is still consistently uneven; with more than 88% of the country having access to power, significant gaps remain between urban and rural areas [5]. Rural electrification rates are significantly lower, especially in the Upper East, Upper West, and Northern regions, where many households continue to experience unreliable electricity supply or lack access to electricity [6]. As a result, a significant proportion of the rural population continues to be energy impoverished, depending on conventional biomass such as firewood and charcoal for cooking and other domestic energy needs [7]. Therefore, the primary challenge to solar adoption in rural areas is not lack of solar energy but rather high upfront capital costs that result in a "poverty premium," paired with geographic isolation that makes grid extension economically unfeasible [8]. Additionally, rural households continue to rely on conventional biomass since standard solar systems are unable to meet the high thermal demands of traditional, intensive cooking methods [9]. The high level of thermal energy needed for cooking is not addressed by standard solar electrification, which mainly supplies low-voltage power for small appliances and evening lights. Therefore, reducing rural energy poverty necessitates a dual approach: the employment of accessible clean-cooking substitutes, like contemporary biomass stoves or LPG, to replace conventional firewood and the deployment of inexpensive electrical energy storage for basic household power [10].

However, relying entirely on clean cooking fuel supply networks presents logistical and financial risks [11]. This highlights the need for a decentralized solar thermal technology, which utilizes the sun's resource for domestic uses [12]. The main challenge of decentralized heating systems is separating solar availability from fluctuating household demand profiles, which remains a primary technological limitation [13]. Resolving this daily disparity using traditional battery-based electrical storage in sub-Saharan climate zones is still expensive, requires regular maintenance, and experiences accelerated thermal degradation because of high ambient temperatures [14]. As a result, latent heat thermal energy storage (LHTES) utilizing Phase Change Materials (PCMs) has become a thermodynamically better alternative to traditional battery-based electrical storage [15][16]. By absorbing solar heat during peak daylight hours and releasing it predictably during periods of high demand, PCMs overcome the limitations of traditional sensible heat storage media. In particular, PCMs use latent heat during isothermal phase transitions to store 5 to 14 times more energy per unit volume, resulting in a greater volumetric energy density [17][18].

Beyond domestic energy requirements, PCM-based solar thermal storage directly tackles post-harvest losses, one of Ghana's most urgent agricultural issues in rural areas. Post-harvest losses in the northern regions are projected to be between 10% and 20% for dry cereals (like maize) and between 10 and more than 40 % for perishable fruits, vegetables, and root and tuber crops (like yams, tomatoes, and mangoes) [19]. These losses, which are caused by insufficient drying, temperature fluctuations, molds, pests, and inadequate storage infrastructure, aggravate food insecurity for smallholder farmers and cause significant financial losses [20][21]. A useful, low-maintenance alternative is offered by PCM thermal energy storage incorporated with solar crop dryers. Without using fuel or grid electricity, the method allows for continuous, regulated drying that quickly lowers moisture content, inhibits microbial development, and prevents spoiling by storing extra daytime solar heat and releasing it gradually during evening or cloudy periods [22][23]. This prolongs shelf life, enhances product quality for market or domestic use, and lowers the 20–50% losses common in conventional open-sun or crude storage techniques employed by rural farmers[24].

Despite the potential of PCM systems for both household thermal needs and agricultural preservation, such designs are not yet widely deployed in sub-Saharan Africa [25] [26]. Their performance has not been adequately optimized for dual-use rural applications or for tropical climatic conditions [27] [28]. This thesis addresses that gap through high-fidelity CFD simulation in ANSYS Fluent, investigating the melting and solidification behavior of PCM in a solar thermal energy storage unit tailored for Ghanaian rural contexts.

1.2 Research Objectives

1.2.1 Main Objective

To numerically investigate and optimize PCM melting and solidification behavior in a solar thermal energy storage system.

1.2.2 Specific Objectives

1. Validate the simulation against well-established experimental benchmark data.
2. Simulate the melting (charging) and solidification (discharging) behavior of selected PCMs.
3. Identify the optimal PCM material and system design configuration for two specific Ghana rural applications: solar cooking and passive food preservation cooling.

Chapter 2

Literature Review

2.1 Cold Storage Systems for Reducing Post-Harvest Losses

Post-harvest losses of fruits and vegetables continue to be a major challenge to food security and rural livelihoods in Ghana and across sub-Saharan Africa [29]. It is estimated that 30% of food is lost before reaching consumers or retailers. Losses for highly perishable horticultural crops are often between 20 and 50% [30, 31]. Figures 2.1 and 2.2 show statistics of global post-harvest losses and the percentage of commodities lost. These losses are mainly caused by lack of cold-chain infrastructure, poor electricity supply in rural areas and poor access to affordable refrigeration [32, 31]. Smallholder farmers dominate production and often lack facilities to maintain the low temperatures required to slow respiration, enzymatic activity and microbial growth after harvest. As such, produce such as tomatoes, mangoes and leafy vegetables deteriorate rapidly under ambient tropical conditions thus decreasing both quantity and nutritional value available for markets and household consumption [32].

Conventional cold storage systems are highly dependent on continuous electrical power and electrochemical batteries when solar photovoltaic (PV) generation is utilized. The cost, maintenance requirements, and short lifespan of batteries are major barriers to widespread deployment in rural off-grid settings [30, 33]. Phase change materials (PCMs) provide an alternative route to thermal energy storage, with the capability to absorb and release large quantities of latent heat during solid–liquid phase transitions at nearly constant temperature [34]. The desired temperature range can be maintained during low or zero solar irradiance by melting and absorbing heat from the storage compartment by incorporating a PCM with suitable melting point in a cold storage unit. This kind of passive discharge ability reduces the battery dependency and improves the autonomy [35].

The use of PCM for agricultural cold storage has been studied in several studies. Numerical and experimental works showed that PCM packs or chambers surrounding a storage volume could maintain the temperatures required for produce preservation during the nighttime or cloudy periods [36, 37]. Similar concepts have been explored in other developing country contexts for portable and containerized cold rooms where the vapor-compression cycle is powered by solar PV during the day to solidify the PCM and the stored latent heat is used to maintain the cold space [36, 38]. The placement of PCM modules affects the thermal uniformity and the completeness of the phase change; configs that maximize the surface contact with the storage air lead to faster and more complete melting or solidification [39, 40].

Numerical modeling is crucial to define the optimal geometry, PCM choice and operational parameters before the expensive construction of a prototype [41, 42]. The enthalpy-porosity method, developed by Voller and Prakash, is a commonly utilized method in commercial CFD packages like ANSYS Fluent for the simulation of solid–liquid phase change [43, 42]. In this fixed grid method, the liquid fraction, 0 for the fully solid state and 1 for the fully liquid state, is calculated in each computational cell using the local enthalpy. The mushy zone is modeled as a porous medium with a porosity equal to the liquid fraction and a momentum sink term proportional to a mushy-zone constant damps the velocity as solidification progresses, effectively

immobilizing the solid region [44, 45]. The method reproduces melting and solidification behavior with acceptable accuracy, provided that the mushy-zone constant is appropriately calibrated (typically between 10^4 and $10^7\,\mathrm{kg\,m^{-3}\,s^{-1}}$) and natural convection is accounted for using the Boussinesq approximation [46, 45], which has been validated against experimental temperature histories and interface evolution.

In ANSYS Fluent, researchers used the solidification/melting model for a variety of latent-heat storage geometries appropriate for cold applications [47]. Simulations of shell-and-tube and rectangular enclosure [47, 48] quantified the effects of fin enhancement, dual-PCM layering and container orientation on solidification time and temperature uniformity. Numerical campaigns in cold-storage contexts have investigated various PCM packet placements and charging/discharging temperature differentials, showing that side-wall or multi-side configurations can attain phase change faster than top- or bottom-only setups, while still maintaining the target air temperature band of approximately 2–6 °C [40]. The studies highlight the sensitivity of performance to the thermophysical properties of the PCM such as latent heat, thermal conductivity, and phase-change temperature range and to the geometric design features that promote heat transfer [34, 49].

Although the number of studies is growing, few have combined detailed CFD modeling of PCM melting and solidification with the specific constraints of solar thermal energy storage units designed for rural Ghanaian conditions. Moreover, the simultaneous investigation of charging under intermittent solar input and passive discharge under realistic ambient heat gains is still underexplored for compact storage units sized for smallholder cooperatives. The present study therefore addresses these gaps by investigating the transient thermal behavior of a PCM based solar thermal energy storage unit for conditions representative of rural Ghana. It thereby provides design insights that can facilitate practical deployment with the aim of reducing post-harvest losses.



Figure 2.1: Effect of socio-economic and infrastructural factors on post-harvest losses of fruits and vegetables. Figure taken from Amjad et al. [30]
[Source].

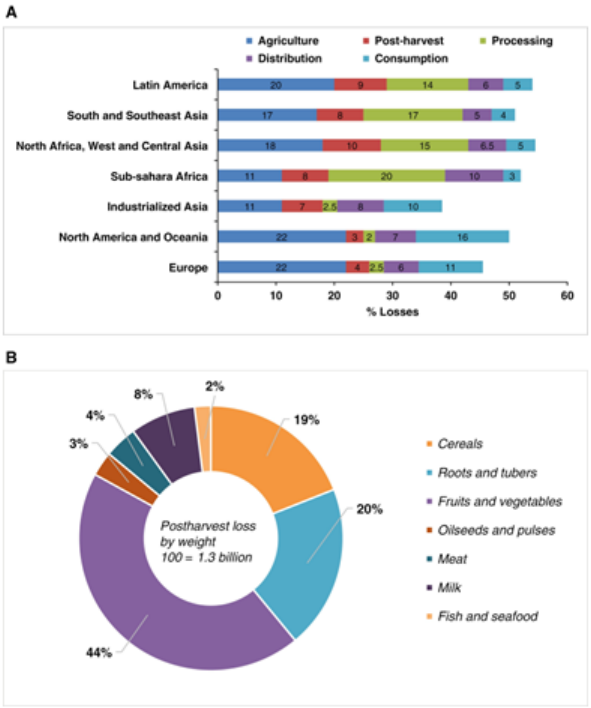


Figure 2.2: (a) Distribution of post-harvest losses of vegetables and fruits in various regions of the world at different stages of supply chain and (b) Percentage of global post-harvest losses by commodity. Figure taken from Amjad et al. [30]
[Source].

2.2 Phase Change Materials (PCMs) for Thermal Energy Storage

2.2.1 Classification of PCMs

Phase change materials [50, 51] are materials that absorb and release thermal energy when changing their phase, usually between the solid and liquid phases. They are capable of maintaining a very narrow temperature range and they can absorb a large amount of heat during melting and give up this heat during solidification, which makes them very useful for thermal energy storage [50, 52]. This behavior has made the study of PCMs for solar thermal applications, water heating, building cooling, food preservation and waste heat recovery [22, 53] widely researched. Depending on their application, phase change behavior and chemical composition, PCMs are classified [54, 55].
Figure 2.3 shows a summary of these classifications.

2.2.1.1 Organic PCMs

One of the dominant classes are organic PCMs [56]. These materials are often stated to be chemically stable and reliable thru multiple temperature cycles [57, 58]. Paraffin waxes are of particular interest in this class since they are readily available, show low phase segregation and are applicable to a range of storage applications [54, 22]. This group also encompasses fatty acids that are often investigated because of their acceptable latent heat values and rather sharp melting temperatures [59, 54]. One of the most common advantages is that organic PCMs are less corrosive than many inorganics [57]. Their main disadvantage is a low thermal conductivity, which is usually responsible for a slow rate of heat charge and heat release [60, 58]. This feature is important in practical systems as it may reduce the overall storage efficiency unless

the methods of heat transfer improvement are introduced.

2.2.1.2 Inorganic PCMs

The second class of PCMs are inorganic PCMs [56]. In broader classifications, some metallic materials are also found, but mostly salt hydrates are representative of these [58, 56] Inorganic PCMs are often reported to possess relatively high latent heat per unit volume and better thermal conductivity than many organic alternatives [57] These features are attractive for compact thermal storage systems. However, the literature often expresses concerns regarding supercooling, phase segregation, and long-term cycling reliability [57, 61, 62]. Such problems may lead to performance degradation after multiple freezing and melting cycles, especially if the material is not adequately stabilized. Therefore, inorganic PCMs might need to be used with additives, nucleating agents, or modified formulations to be effectively applied in storage units [62].

2.2.1.3 Eutectic PCMs

Another class consists of eutectic PCMs. They are mixtures that are designed to melt and freeze at a certain temperature different from the individual components [63]. Eutectics are useful because they allow researchers to fine tune phase change temperature for a specific application [64]. This can be beneficial in systems where the storage material has to operate within a narrow thermal window. This design flexibility makes eutectic materials promising, although their practical use still depends on thermal stability, compatibility with the container and cost [65]. Not just descriptive but also helps in selection of materials . Classification of PCMs . The thermal behavior of a PCM is studied by researchers in relation to the operating conditions of the system. For solar cooking, a PCM needs to have a melting temperature sufficiently high to store useful cooking heat whereas for cooling or preservation, the melting temperature should be close to the desired storage temperature [66].

Classification is important for this study because the choice of PCM must respond to Ghana's thermal needs and climatic conditions. Para- fin grades and fatty-acid based materials are often investigated for high temperature applications such as solar assisted cooking or hot water storage due to their stability and ease of handling [67]. Salt hydrates or lower melting paraffins may be considered where appropriate for low-temperature applications such as food preservation [58]. The literature clearly states that the PCM classification is directly related to the application temperature, the desired storage duration and the practical conditions under which the storage unit will operate [62, 68]. This calls for a more complex approach to PCM selection, that moves beyond broad classifications to a more granular assessment of the thermophysical properties within specific operational envelopes.

2.2.2 Thermophysical Properties of PCMs

The performance of PCM is greatly influenced by its thermophysical properties. These properties control not only how much energy the material can store, but also how fast that energy can be absorbed and released. The first property considered in most PCM studies is the phase change temperature. This temperature should be in the operating range of the application. If the melting point is too low, the material may not release enough useful heat on discharge. If it is too high the available heat source may not be able to melt it completely. Therefore, temperature matching is often seen as the most important criterion in selection.

Another important property is the latent heat of fusion. This quantity is the energy absorbed during melting or released during solidification [69]. A high latent heat value is desirable so more energy can be stored per unit mass [22]. In practice, this reduces the required amount of PCM for a given duty [54]. However, a PCM with good mass-based latent heat but low density might still need large containment volumes which might limit its applicability in space-constrained designs.

Another property which has received considerable attention in the literature is thermal conductivity [22]. Many PCMs, especially organic PCMs, have low thermal conductivity [70]. This slows down the movement of heat into the material when charging and out of the material when discharging. Thus, high storage capacity materials could perform badly if the heat transfer rate is too low [22, 70]. This is one of the main reasons

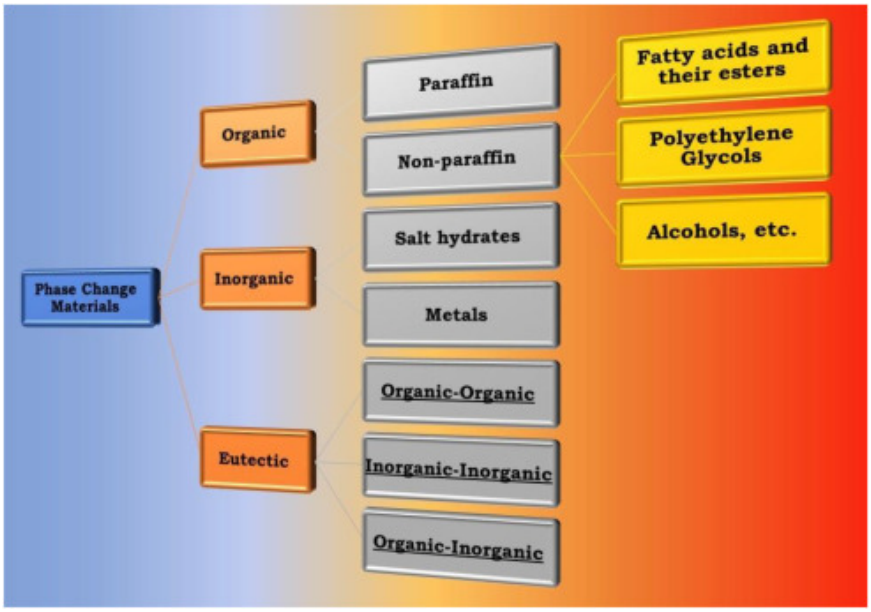


Figure 2.3: PCM Classification. Figure taken from Majd et al. [Source].

why fins, metal foams, graphite additives and modified geometries are studied from researchers. Thermal conductivity is a critical parameter in CFD studies that directly affects the predicted temperature fields, melt-front development and charging time [70].

The specific heat capacity is also relevant for the PCM behavior [54]. The main characteristic is the storage of latent heat but before the melting starts and after the solidification is done, the sensible heat is also stored [22]. A phase change material with a good specific heat can provide additional energy storage outside the phase change interval. This can improve the overall thermal response of the system, especially when the operation temperature varies around the melting point [54].

The PCM density affects the system design and the natural convection behavior during melting [54]. In numerical modeling, the variation of density with temperature is often a factor influencing buoyancy-driven flow in the liquid phase. This is important because in some parts of the container natural convection can significantly speed up melting while in other parts it will have negligible effect.

Researchers also investigate the volume change, thermal stability, and cycling reliability [70]. Many PCMs expand upon melting and contract upon solidification [54]. Failure to account for this change can result in mechanical stress on the container or leakage issues [61]. Thermal stability is the capacity of the material to maintain its properties thru repeated use. A PCM that deteriorates, separates, or exhibits greater supercooling over time may not be appropriate even if its initial properties appear promising [70]. In rural energy systems where the chances for maintenance may be limited, long-term reliability is of particular importance.

Another important issue is sub-cooling (or supercooling). This is when a PCM is still liquid below its usual freezing point and delays the heat release [71, 72]. In storage systems, the subcooling can decrease the discharge performance as the expected crystallization process does not start at the expected temperature. The problem is more common in some inorganic materials [65] and is often discussed together with phase segregation, which also reduces heat storage capacity due to irreversible separation of constituents [72].

Literature also stresses the need to measure thermophysical data accurately. Properties such as melting

temperature, latent heat, conductivity and specific heat are not always constant and can depend on purity, formulation or testing method [73, 74]. Differential scanning calorimetry (DSC) is a commonly used technique for characterizing small samples, while the T-history method is often recommended for larger or more representative samples [75, 76]. Simulation-based work is sensitive to property data, and inaccurate property data results in large errors in melt-fraction prediction, thermal response time and stored energy estimation [76].

The comparison of materials in this thesis is focused on thermophysical properties. A PCM for preservation or passive cooling must operate in a lower temperature range and provide a stable discharge over long periods of time. It is evident from the literature that no material should be selected on the basis of a single property. The selection must be based on the joint impact of temperature, storage capacity, conductivity, stability and compatibility with the design of the storage unit [65, 54, 72].

2.2.3 Principles of Latent Heat Storage

Latent heat storage means the uptake or release of energy during a phase transition [54, 72]. This transition is between the solid and liquid phases in most of the thermal energy storage systems involving PCMs [77, 72].

During charging process, the heat from an external source is transferred into the PCM [77, 54]. The temperature of the solid PCM rises sensibly, in the beginning, until the phase change interval is achieved. Once melting starts the material takes in a lot more heat without a significant temperature rise [77, 72]. This energy is stored in the liquid phase and can be recovered during discharge. See Figure 2.4.

During discharge it is just the reverse process. The PCM, now a liquid, begins to lose heat and solidify. As the solidification proceeds, the latent heat is released to the surrounding medium. This property enables PCMs to deliver heat at nearly constant temperature for a useful duration [78]. In solar applications this behavior is very advantageous as the heat source is intermittent. Sunlight is strongest during the day, but household and agricultural demand can extend to the evening and nite. As such a PCM storage unit forms a thermal buffer between energy availability and energy demand.

Literature usually distinguishes between latent heat storage and sensible heat storage. In sensible systems, the only way to store energy is to raise the temperature. The mass of the material and the specific heat capacity and the change in temperature allowed determine the amount of storage. In latent systems, much of the stored energy is associated with the phase transition itself. This allows for much higher storage densities in a narrower temperature range. As such, PCMs are commonly suggested as a more compact option compared to water tanks or rock beds for applications where space and thermal regulation are key [79].

The thermal behavior in a PCM storage unit is complex. Conduction is dominant at the beginning of melting, particularly near the heated wall. The formation of more liquid PCM causes buoyancy-driven natural convection in the melted region. This liquid motion redistributes heat, and can accelerate melting in the upper parts of the container while the lower parts are less advanced, giving a non-uniform melting front. Convection is less important during solidification as the growing solid layer stops fluid movement and conduction takes over. This results in a slower solidification than melting and in imbalances in charge and discharge performance [80].

These heat transfer limitations have led to the development of performance enhancement techniques for latent heat storage systems. One of the most utilized methods is fins, as they increase heat transfer area and decrease the conduction path inside the PCM [81]. Shell and tube designs, encapsulation, porous matrices and conductive additives are also widely investigated. The literature indicates that the performance of a latent heat storage unit depends not only on the PCM selection but also on the design features that control the heat transfer within the unit.

The principles of latent heat storage are of direct relevance for solar thermal systems [82]. A solar collector can charge the PCM during the hours of high irradiation; the stored energy can be released when required [72]. In solar cooking, the heat stored can be released in the late afternoon or evening when there is high demand for cooking [83]. The stored thermal effect can help to keep temperatures under control during the night for preservation or cooling applications.

The ability to modulate thermal availability over time makes PCM-based latent heat storage very attractive for rural applications in places like Ghana where solar energy is abundant in the day but the need for thermal energy (cooking, hot water, crop drying) occurs later. Direct thermal solutions for the intermittency of solar energy provided by PCM storage can be costly and require maintenance for battery systems in remote locations [72, 84].

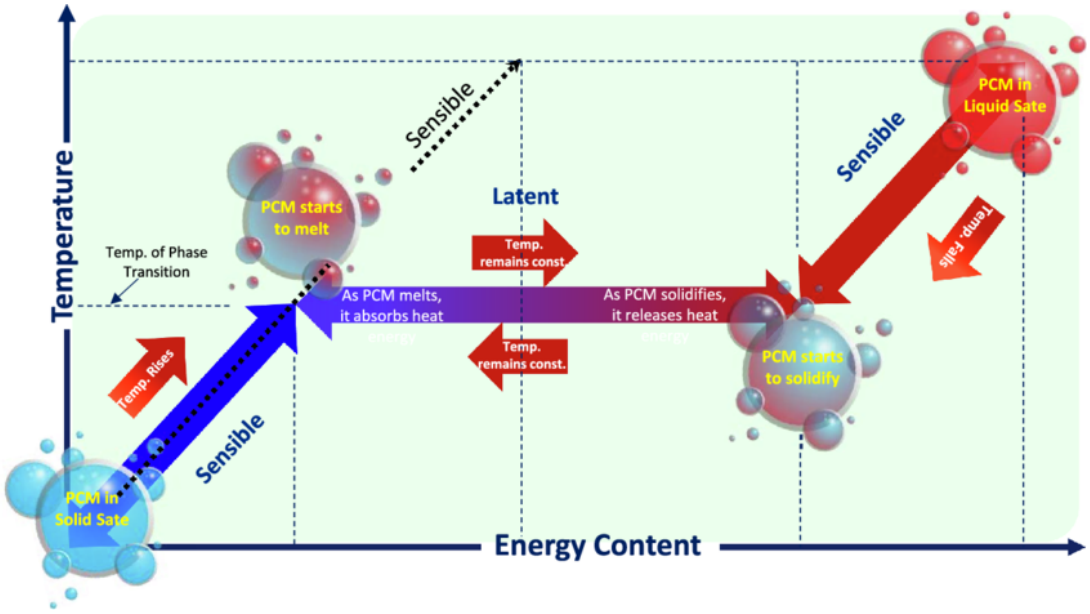


Figure 2.4: PCM Classification. Figure taken from Khan et al. [72] [Source].

2.3 CFD Modeling of PCM Systems

The melting and solidification processes are characterized by coupled heat transfer, fluid motion and a moving phase boundary that are difficult to fully capture by experiments alone. For this reason, computational fluid dynamics has become one of the main tools for the study of phase change material systems [85]. In PCM storage units, the temperature field is always changing with time, the liquid fraction varies from cell to cell, and the natural convection in the molten region can significantly change the shape of the melt front [81, 62].

CFD is useful in this context: researchers can visualize these internal processes and quantify the effect of design variables like geometry, fin arrangement and boundary conditions on charging and discharging performance. Recent review studies confirm that CFD is now widely used in latent heat thermal energy storage research, especially in work where convection has a strong influence during melting [86].

The major numerical difficulty of PCM modeling is the treatment of the solid-liquid interface. Classical phase-change problems are of the Stefan type, where the location of the interface is not known a priori and must be obtained as part of the solution. Over the years, several numerical schemes have been developed

to overcome this difficulty. Most existing studies differentiate between interface-tracking methods, interface-capturing methods and fixed-grid approaches. Fixed-grid methods are particularly popular for engineering applications, since they do not require remeshing and are easier to implement in commercial packages. This is why a large proportion of the applied PCM work, including studies of solar thermal storage, relies on fixed-grid enthalpy formulations [87].

The enthalpy-based formulation has become the leading method among fixed-grid methods [87]. In this approach, latent heat is incorporated into the energy equation as an enthalpy term, so that the phase-change process can be modeled without explicit treatment of the interface. The foundation work of Voller and Prakash was a major influence in the simulation of PCM, and later the enthalpy-porosity technique developed by Brent, Voller and Reid [88]. In the enthalpy-porosity model, each control volume is assigned a liquid fraction and the mushy region is treated as a porous region where the velocity is gradually reduced as the material solidifies. This allows latent heat effects and natural convection to be simulated on a single computational grid at a reasonable computational cost.

The importance of the enthalpy-porosity model is closely related to its use in the validation of benchmark problems. One of the most well known cases is the melting of gallium in a rectangular cavity, heated from one vertical side, first reported by Gau and Viskanta [89]. The results of that study clearly pointed out that natural convection plays an important role on the shape of the solid-liquid interface, especially in the upper region of the enclosure. It provided a detailed description of the development of the interface and temperature behavior and therefore became a reference case for checking the ability of numerical models to reproduce realistic melt-front evolution. Even recent PCM studies still use the gallium problem to test mesh sensitivity, time-step effects and the influence of mushy-zone constants [90].

A major strength of CFD in PCM research is the capability to resolve natural convection during melting. Pure conduction models may be adequate in idealized setups, but in real storage units these models often become inadequate because of density differences in the liquid phase that generate buoyancy-driven flow [91]. This flow promotes melting near the top of a cavity, while the lower regions melt slower, resulting in a non-uniform interface and temperature field [92, 81]. Therefore, CFD models that consider momentum transport are necessary when the goal is to understand real melting behavior, not just to estimate total stored energy [85, 91]. This is especially true for solar thermal units, where charging is often under transient boundary conditions and the rate of delivering heat is as important as the total capacity [93].

Commercial software has had a very large role in the spreading of PCM CFD analysis. One of the most popular platforms is ANSYS Fluent which features an in-built solidification and melting model using the enthalpy-porosity method [94, 95]. This has made Fluent attractive for researchers to investigate cavities, shell-and-tube systems, finned containers or encapsulated PCM arrangements without the need to develop a custom solver [95]. The frequent use of Fluent in published studies has also built up a body of similar numerical practice, which is useful for thesis work that is seeking to follow the accepted validation procedures and parameter studies [96, 97].

Despite the wide acceptance of the enthalpy-porosity model, the numerical accuracy strongly depends on the modeling choices. The mesh density impacts the prediction of the melt front and the temperature gradients and the size of the time-step impacts the stability and the transient accuracy of the solution [98, 99]. The quality of the results can also be affected by the choice of discretization scheme and convergence criteria. Another sensitive parameter is the mushy-zone constant which controls the amount of momentum suppression in partially melted cells[100, 101]. If it is set too low, unrealistic velocity may appear in regions that are almost solid. If it is set too high, fluid motion may be overly damped [102] . Recent analyzes of the gallium melting problem show that such differences can significantly alter melt-fraction histories and interface shape. Therefore, mesh-independence studies and prudent selection of parameters remain of utmost importance [103].

CFD has also become central to design-oriented studies of PCM thermal storage. This study provides a simple and effective way to study the impact of fins, aspect ratio, wall heat flux, PCM thickness, tube

placement and encapsulation design on the charging rate and heat recovery without the need for physical experiments for every design variation in terms of cost and time. This is especially useful in solar thermal storage, where the storage unit is often to be tuned to a specific duty, for example evening cooking, domestic hot water buffering or overnight cooling.

Chapter 3

Mathematical Model and Numerical Method

3.1 Mathematical Formulation

A mathematical framework is required for numerical simulation of phase change material (PCM) melting and solidification to describe accurately the coupled thermal and fluid dynamic phenomena during phase transition process. This chapter provides the governing equations and modeling assumptions, and enthalpy-porosity method employed in simulation of the PCM thermal energy storage unit by ANSYS Fluent.

3.1.1 Governing Equations

The numerical model of PCMs melting and solidification is based on the basic principles of fluid mechanics and thermodynamics. The following assumptions are adopted to simplify the governing equations without loss of physical accuracy:

- The liquid phase is assumed to be incompressible.
- The buoyancy driven natural convection is modeled by Boussinesq approximation where the density variation is considered only in the body force term of the momentum equation.
- The flow in the melt region is assumed to be laminar.
- Viscous dissipation effects are considered negligible.

Under these assumptions the governing equations of mass, momentum and energy conservation in the PCM domain are presented in the following subsections.

3.1.1.1 Continuity Equation

The continuity equation enforces conservation of mass within the fluid domain. For an incompressible fluid, the divergence of the velocity field is zero. This is expressed as:

$$\nabla \cdot \vec{v} = 0 \tag{3.1}$$

where $\vec{v}$ is the velocity vector of the liquid PCM [104].

3.1.1.2 Momentum Equation

The momentum equation describes the conservation of linear momentum within the liquid PCM. The general form of the Navier-Stokes equation for an incompressible Newtonian fluid is:

$$\rho \left(\frac{\partial \vec{v}}{\partial t} + (\vec{v} \cdot \nabla)\vec{v} \right) = -\nabla P + \mu \nabla^2 \vec{v} + \rho \vec{g} + \vec{S} \tag{3.2}$$

where ρ is the fluid density, P is the pressure, μ is the dynamic viscosity, $\vec{g}$ is the gravitational acceleration vector, and $\vec{S}$ is a source term [105].

3.1.1.3 Energy Equation

The energy equation governs the distribution of thermal energy within the PCM domain. The governing enthalpy equation is expressed as:

$$\rho\frac{\partial H}{\partial t} + \rho\nabla\cdot(\vec{v}H) = \nabla\cdot(k\nabla T) + S_h \tag{3.3}$$

where H is the total volumetric enthalpy, k is the thermal conductivity, and S_h is any additional heat source term.

The total enthalpy is decomposed as:

$$H = h + \Delta H \tag{3.4}$$

where the sensible enthalpy is:

$$h = h^{\text{ref}} + \int_{T^{\text{ref}}}^{T} c_p\, dT \tag{3.5}$$

and ΔH is the latent heat content. [104, 105]

3.1.2 Enthalpy-Porosity Method

The enthalpy-porosity method treats the phase transition region (mushy zone) as a porous medium whose permeability varies with the local liquid fraction. This approach is implemented in ANSYS Fluent for the PCM simulations in this study.

3.1.2.1 Liquid Fraction

The liquid fraction β is defined as:

$$\beta = \begin{cases} 0, & \text{if } T < T_{\text{solidus}} \\ \dfrac{T - T_{\text{solidus}}}{T_{\text{liquidus}} - T_{\text{solidus}}}, & \text{if } T_{\text{solidus}} \le T \le T_{\text{liquidus}} \\ 1, & \text{if } T > T_{\text{liquidus}} \end{cases} \tag{3.6}$$

For materials that melt over a temperature range (most commercial PCMs), β is usually assumed linear between the solidus and liquidus temperatures [104, 105].

3.1.2.2 Mushy Zone Modeling

The Carman-Kozeny Equation;

$$\vec{S} = -A_{\text{mush}}\left[\frac{(1-\beta)^2}{\beta^3 + \varepsilon}\right]\vec{v} \tag{3.7}$$

where A_{mush} is the mushy zone constant and ε is a small number (typically 0.001) to avoid division by zero.

A sensitivity analysis of the mushy zone constant A_{mush} was performed to ensure accurate representation of the melting behaviour and good agreement with benchmark data [104].

3.2 Simulation Procedure

The procedure for the studying the melting and solidification process of PCM in ANSYS follows several steps, which is demonstrated in the flowchart in figure 3.1.

Initially, the geometry of the PCM domain is prepared using DESIGN MODELER software in Ansys Workbench and named selections are done for each face. Then, the computational mesh is generated in Ansys Meshing (mechanical) software. Numerical analysis of the heat transfer is based on the governing equations (continuity, momentum and energy equations). The flow is assumed to be laminar, and the thermophysical parameters are assumed to be constant. The model is compared with Gau and Viskanta's experimental work on gallium melting.

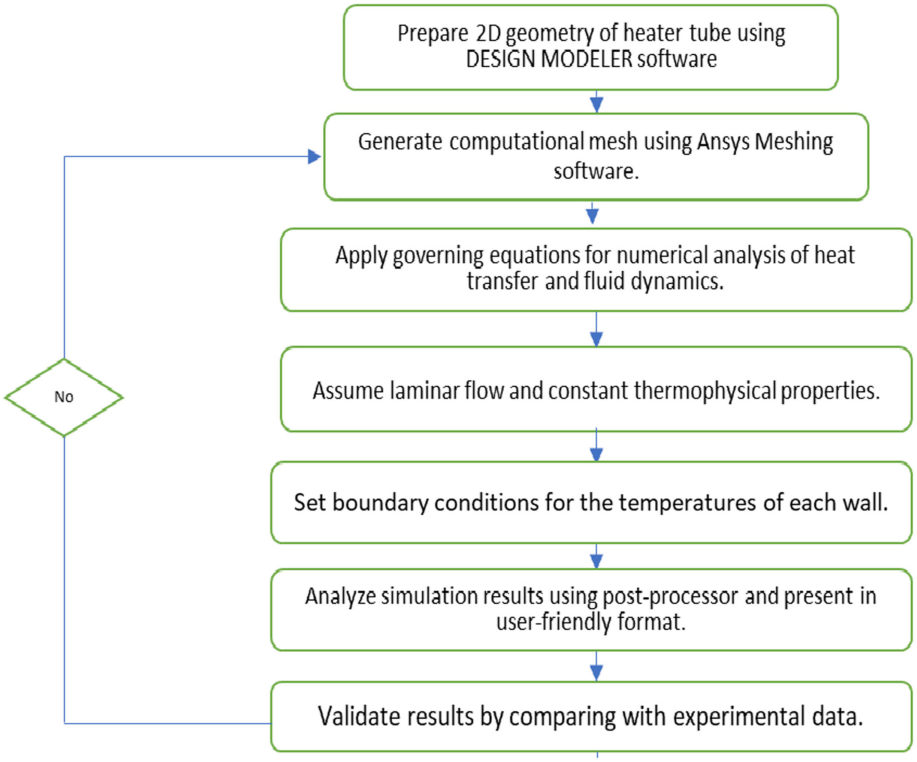


Figure 3.1: Simulation procedure for PCM melting

3.3 Geometry and Computational Domain Setup

The accuracy and reliability of any computational fluid dynamics (CFD) simulation depends heavily on the fidelity of the geometric model and the quality of the computational mesh. The geometry of the phase change material (PCM) thermal energy storage unit was constructed and discretized in this study using ANSYS Fluent 2026 R1. The computational domain was modelled to mirror the physical arrangement of a passive food preservation cooling system designed for rural use in Ghana.

3.3.0.1 2D Geometric Description

The food preservation system was modelled as a rectangular two-dimensional PCM panel. The domain is a flat PCM slab contained within a rectangular enclosure, a configuration suitable for passive cooling applications where the PCM panel is integrated into the walls or base of a food storage unit. The rectangular geometry was chosen for its large heat-transfer surface area, the ease of uniform charging and discharging behaviour, and the ease of parametric investigation of the effect of aspect ratio and layer thickness.

Gravity was applied in the y-direction with a gravitational acceleration of $-9.81\,\mathrm{m/s^2}$ to allow for buoyancy-driven natural convection inside the melt region.

Four boundary conditions were applied to the walls of the rectangular domain as shown in 3.2. Each boundary was treated as a wall with the following thermal conditions:

- **Left wall (hot wall):**A constant temperature boundary condition of 309 K (35.85 °C) was imposed. This mimics the hot ambient environment driving the melting (charging) of the PCM.
- **Right wall (cold wall):** The boundary condition of constant temperature 288.2 K (15.05°C) was applied. This is the solidus temperature of RT18 and the cooled boundary driving solidification (discharging).
- **Top wall:** An adiabatic boundary condition
- **Bottom wall:** An adiabatic boundary condition

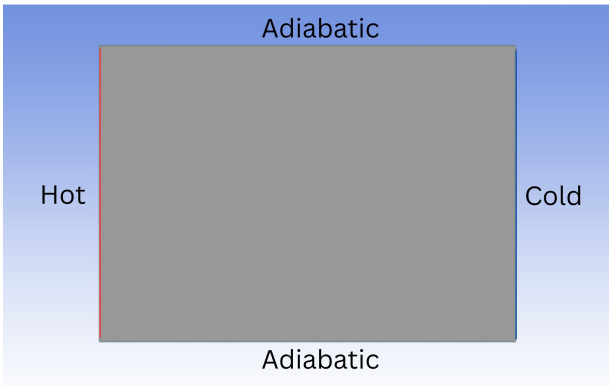


Figure 3.2: 2D Geometry and Boundaries

The asymmetric thermal boundary conditions (warm left wall at 309 K and cooled right wall at 288.2 K) establish a horizontal temperature gradient across the PCM slab. This drives melting from the left boundary toward the right and induces buoyancy-driven natural convection within the liquid melt region. The top and bottom adiabatic walls ensure that energy exchange occurs exclusively through the lateral surfaces.

The computational mesh for the rectangular PCM panel was generated using ANSYS Fluent's meshing tools, employing a structured quadrilateral mesh. A structured mesh was chosen for its superior numerical accuracy, high orthogonal quality, and efficiency for the simple rectangular geometry.

Statistics	
Nodes	3721
Elements	3600
Show Detailed Statistics	No

Figure 3.4: Mesh Statistics

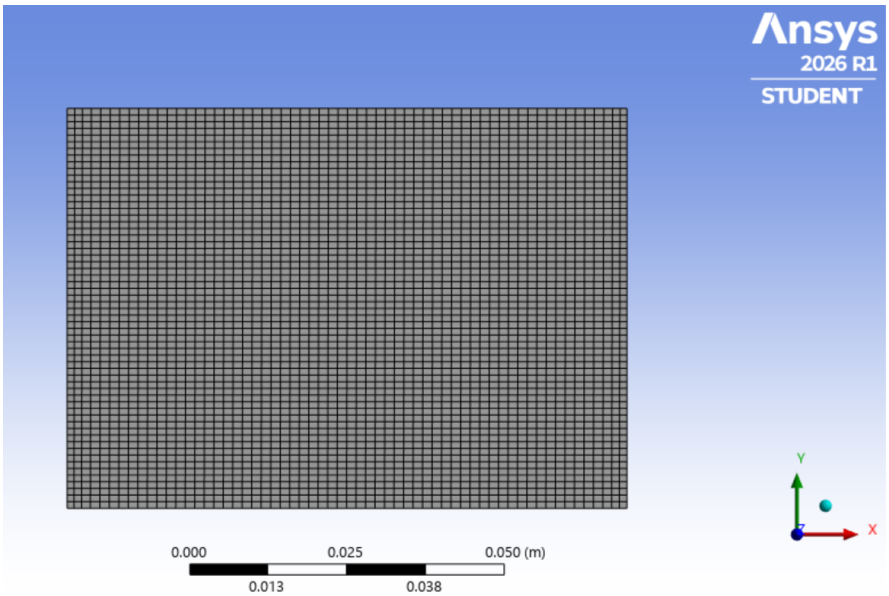


Figure 3.3: 2D Mesh

The near-unity orthogonal quality and low aspect ratio confirm excellent mesh quality, with no warnings or failures in the Mesh Quality Worksheet. A mesh sensitivity study was performed and the mesh with 3,600 elements was used for all further simulations after checking the mesh-independent results.

3.3.0.2 PCM Material Selection and Properties

The thermophysical properties of RT18, as entered into the ANSYS Fluent material database, are summarised in Table 3.1.

Table 3.1: Thermophysical properties of Paraffin RT18 as used in the ANSYS Fluent simulation.

Property	**Value**	**Unit**
Density	880	kg/m^3
Specific Heat Capacity (c_p)	2000	J/(kg·K)
Thermal Conductivity (k)	0.2	W/(m·K)
Dynamic Viscosity (μ)	0.004–0.005	Pa·s
Solidus Temperature	288.2	K (15.05°C)
Liquidus Temperature	290.2	K (17.05°C)
Latent Heat of Fusion	174	kJ/kg
Density Model	Boussinesq	—

The density of RT18 was modelled using the Boussinesq approximation. The specific heat capacity and thermal conductivity were treated as constant.

3.3.0.3 Initial Conditions and Domain Initialisation

The simulation was initialised using the standard initialisation method in ANSYS Fluent. The initial velocities in both the x and y directions were set to zero and the initial gauge pressure was set to zero.

First, the PCM domain was patched with a temperature of 286.2K (13.05°C), which is below the solidus temperature of RT18, ensuring that the domain is initially fully solid. The simulation is run in transient mode with pressure based solver. Based on the sensitivity analysis, the constant for the mushy zone was set to 100,000.

3.3.0.4 3D Geometric Description

For the application part, 3D geometry was generated as shown in 3.5. The geometry is made up of an outer insulation box, which contains 5 PCM plates. Figure 3.6 shows the meshing grid of the five PCM arrangements and Figure 3.7 shows the meshing grid of the outer insulation. The insulation box has an outside dimension of 430mm (Length)× 285mm (Width) 345mm (Height) and an inside dimension of 355mm (L) × 215mm (W) × 265mm (H).

3.3.0.5 Materials and Methods

Rubitherm RT8 was chosen as the PCM for the numerical investigation for the cold storage application. The thermophysical properties of the PCM used in the simulation are taken from [106] The PCM was selected based on its melting temperature range suitable for low-temperature thermal storage applications.

The computational domain was a PCM storage region inside an insulated container. ANSYS Workbench was used to build and mesh the geometry and the PCM region was meshed using an unstructured mesh. Transient numerical simulations were performed in ANSYS Fluent. The melting process of the PCM was modeled by the enthalpy-porosity method. The phase transition was modeled in the terms of the liquid fraction and the latent heat contribution in the energy equation. The mushy zone was modeled as a porous medium and the momentum source term was used to decrease the velocity as solidification progresses. A mushy zone parameter of 10e5 was applied.

The PCM melting process was simulated under transient conditions with the appropriate thermal boundary conditions imposed on the storage enclosure. The SIMPLE scheme was initially considered but the PISO algorithm was applied to achieve a better stability of the solution due to convergence problems. The pressure-based solver was adopted with the second-order implicit time discretization for the improvement of transient solution accuracy. The timestep was 0.01s. To solve the divergence problems, the under-relaxation factors were modified, the boundary conditions were refined and the simulation parameters were adapted.

The evolution of the PCM temperature and liquid fraction and their residual values were used to monitor the solution convergence. At the beginning, the simulations showed a small variation in the temperature of the PCM and the liquid fraction. However, after tuning the numerical settings, an increase in the PCM's temperature and the melting process was observed. The heat transfer and the temperature evolution at different simulation times were recorded to evaluate the thermal response of the storage system.

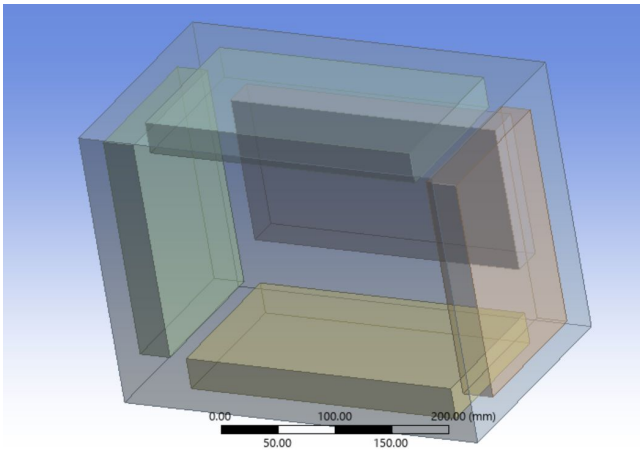


Figure 3.5: 3D Geometry of cooling storage

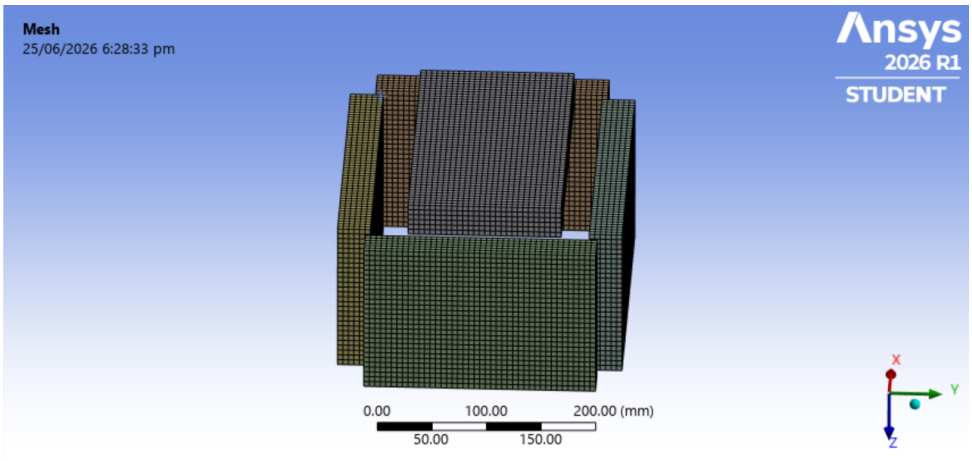


Figure 3.6: 3D Meshed geometry of PCMs

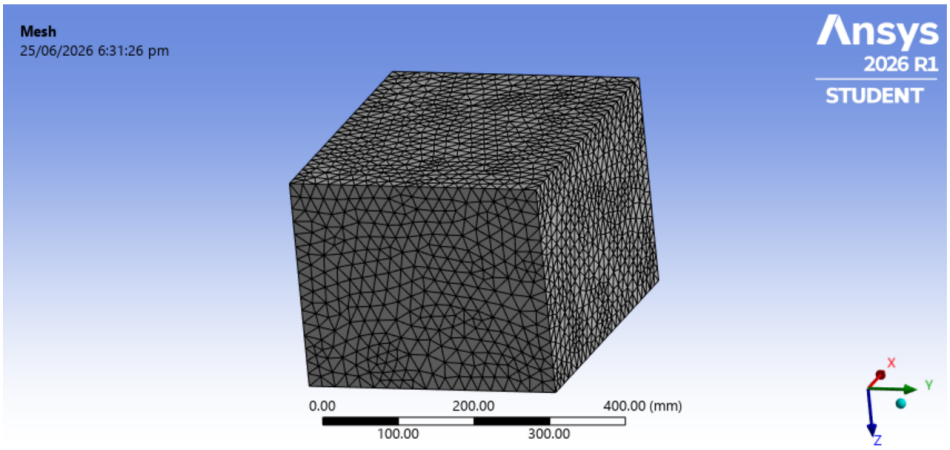


Figure 3.7: 3D Meshed geometry of insulation

3.3.1 Mesh Independence Study

To study the effect of spatial discretization on the predicted melting behavior of PCM, the mesh independence analysis was carried out using two different mesh sizes of 1.5 mm and 1.3 mm. The comparison was made on the basis of the evolution of liquid fraction and temperature with time. The simulations were performed using the same boundary conditions and solver settings, and the liquid fraction and temperature history were taken from the PCM domain.

The time evolution of the liquid fraction for the two meshes is shown in Figure 3.8. The results indicate that both meshes predict a similar melting trend for the entire simulation time. As the heat is transferred to the PCM the liquid fraction increases steadily with only small differences between the two mesh resolutions. As the melting proceeds, the predicted values of liquid fraction are almost the same, which means that the further mesh refinement does not significantly affect the phase transition prediction.

Figure 3.9 shows the temperature variation obtained from the two mesh configurations. Similar trend is observed and both meshes capture temperature increase through melting process. The difference between the two cases is small during the whole simulation period. The temperature profiles show the same trend and converge to a similar final value, which indicates that the mesh resolution used is sufficient to adequately

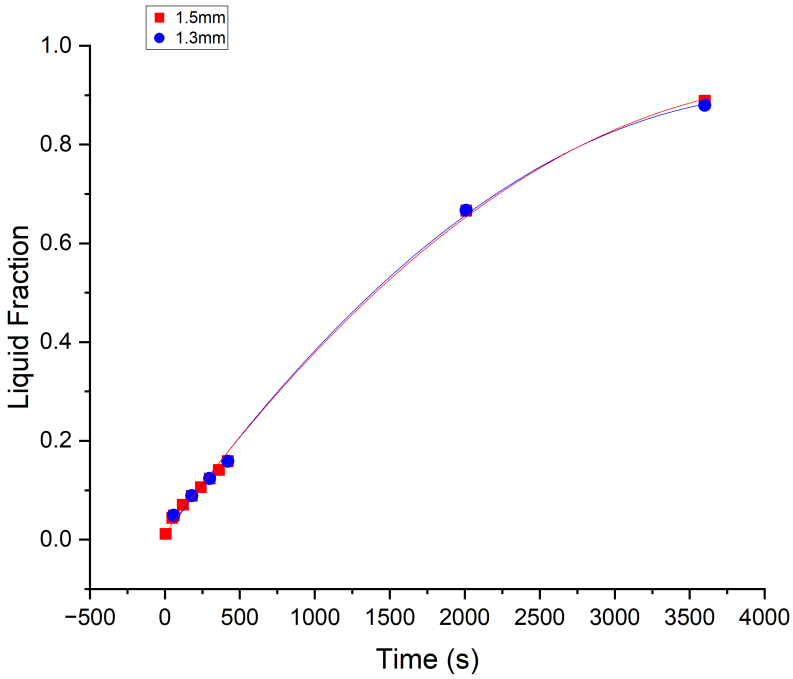


Figure 3.8: Liquid fraction versus time

capture the thermal response of the PCM.

Comparison of the two mesh resolutions shows that the change of element size from 1.5 mm to 1.3 mm only causes a small change of the liquid fraction and temperature prediction. The discrepancy between the two solutions is still in an acceptable range. This shows that the numerical results do not depend on further mesh refinement. Afterwards a mesh size of 1.3 mm was selected as it is providing an increased spatial resolution with reasonable computational requirements.

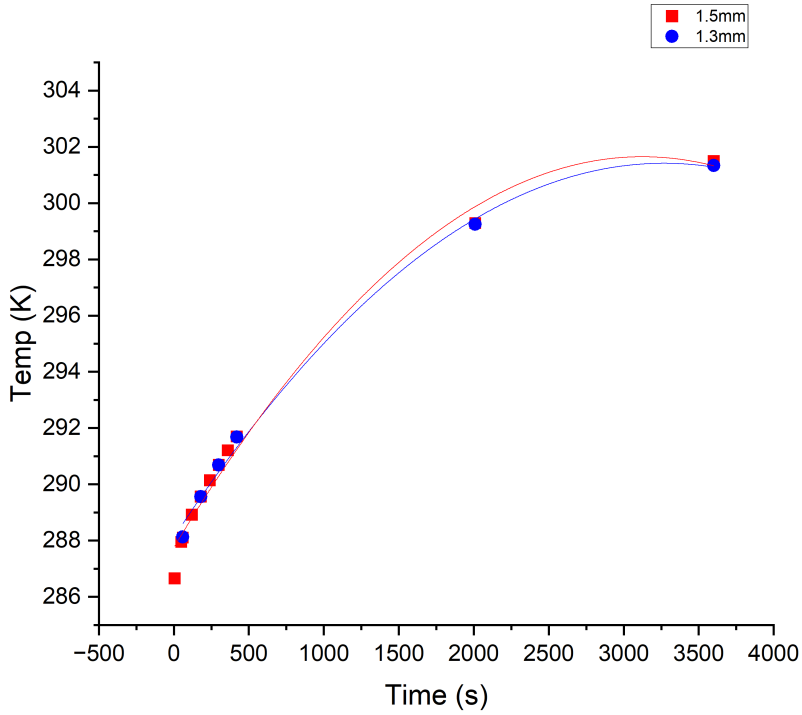


Figure 3.9: Temperature versus time

Chapter 4

Model Validation

4.1 Benchmark Validation

Since the scope of this work did not include experimentation, the experimental work of Gau and Viskanta ([107]) was used to validate the model. Gau and Viskanta (1986) conducted an experiment using gallium with a 99% purity and 29.78 °C fusion temperature and monitored the melting process of the gallium. They selected gallium because it had a well esiablished thermophysical property. Figures 4.1 and 4.2 show the schematic of the test cell used for the experiment. The experiment was conducted by keeping the temperature in the test cell constant such that only one phase of the gallium existed. A constant temperature was achieved by circulating fluid with a constant temperature through two heat exchangers connected to the test cell. To initiate melting or solidification, the temperature of one of the heat exchangers is changed. The interface of the melt was measured using the pour-out and probing method. At specific times, the phased-change process was paused, and the liquid was drained. After that, the solid-liquid interface position was photographed.

To validate this model, properties of gallium as specified in [107] were used, and the geometry was constructed with an aspect ratio of 0.714 as specified in Gau and Viskanta's work. In fluent, gravitity was activated with a value of $9.8m/s^2$. The solidification and melting model was turned on and 10^5 mushy zone parameter was applied. Since the velocity of the liquid phase is minimal, the laminar model was implemented.

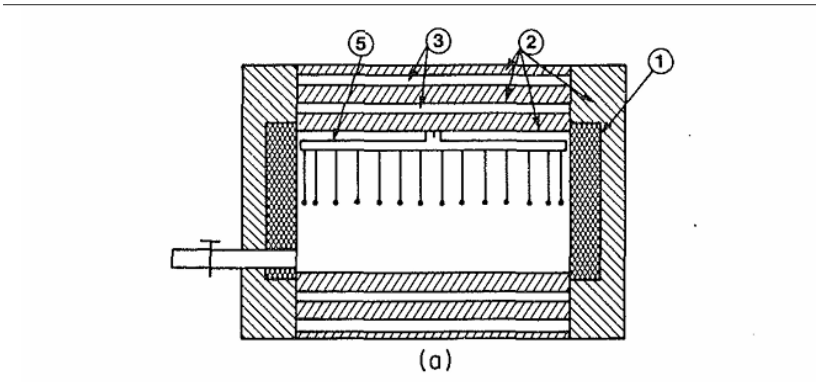


Figure 4.1: Front view of test cell
[Source]

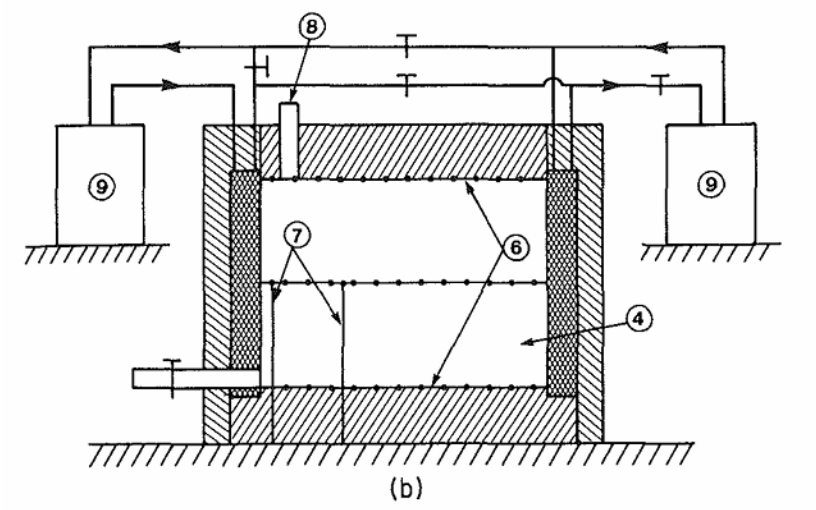


Figure 4.2: side view of test cell
[Source]

(1) heat source and/or sink, (2) Plexiglass wall, (3) air gap, (4) phase change material, (5) thermocouple rack, (6) thermocouples along the walls, (7) small-diameter thermocouples, (8) hole for filling material, and (9) constant temperature baths [107].

4.1.1 Comparison of Melting Interface Positions

The numerical model was validated by comparing the predicted melting behaviour with the experimental results of Gau and Viskanta for melting of gallium in a rectangular cavity. This experiment is a standard benchmark case for phase change simulations as it shows the effect of natural convection on the evolution of the solid-liquid interface. The comparison was carried out with the contours of the liquid fraction at different melting times.

Numerical results show that at the beginning of melting, melting process starts near the heated vertical wall and a thin liquid layer is formed and the rest of PCM is still in solid state. This behaviour is in agreement with the experimental observation where the first phase transition is mainly driven by heat conduction through the solid PCM. The predicted melting front is still roughly vertical in this stage, which indicates the model is correctly predicting the initial heat penetration into the PCM.

The numerical results reproduce the change in the shape of the solid-liquid interface observed experimentally with the progress of melting. The liquid phase reaches the top in about 2-3 minutes and the melting front is more curved as shown in Figure 4.4. This change occurs because the melted PCM adjacent to the heated wall is subject to buoyancy effects, which causes the warmer liquid PCM to rise and cooler liquid to move downward. The natural convection flow increases the heat transfer in the upper part of the enclosure and causes a non-uniform melting rate. The experimental curves of Gau and Viskanta show the same behavior where the melting front advances faster in the upper region than in the lower region.

The numerical model predicts that, at later times, the melting interface would move further to the right side of the enclosure. The simulated contours indicate that the upper part melts faster than the lower part, resulting in an inclined and curved interface. This is consistent with the experimental results which show that the convection effect increases as the liquid region increases. The similarities in the interface shape and evolution suggest that the enthalpy-porosity model is able to correctly model the interaction between the latent heat transfer and the buoyancy driven flow.

The numerical and experimental results are compared and show a good qualitative agreement in the whole process of melting. The model reproduces the main features of the PCM melting including the initial conduction-dominated stage, the onset of natural convection and the upward acceleration of the melting front. The small differences between numerical and experimental interfaces can be attributed to the differences in experimental conditions and numerical assumptions. Constant thermophysical properties were used in the simulation, whereas in the experimental system there may be temperature-dependent variations in density, viscosity and thermal conductivity.

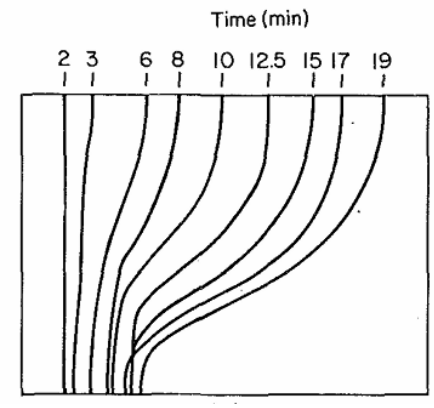
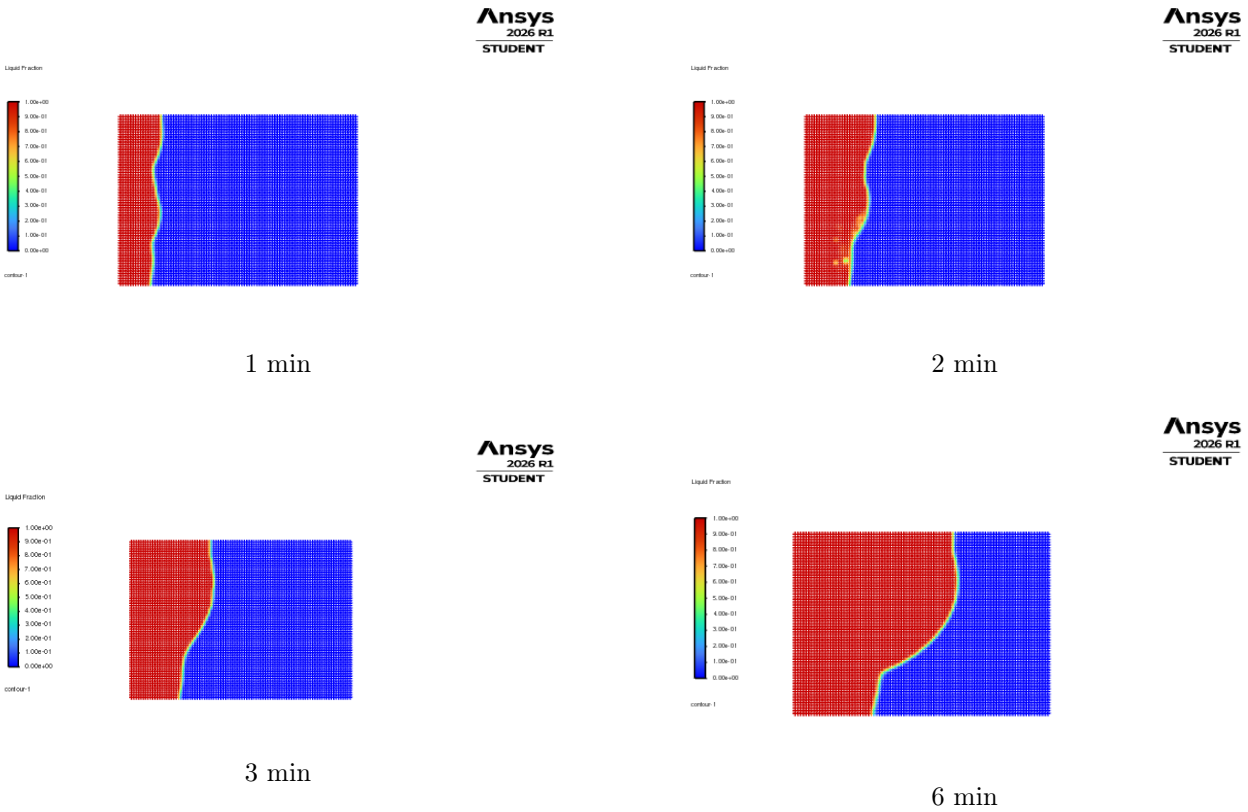


Figure 4.3: Gau and Viskanta experimental interface positions at different times [Source]



1 min

2 min

3 min

6 min

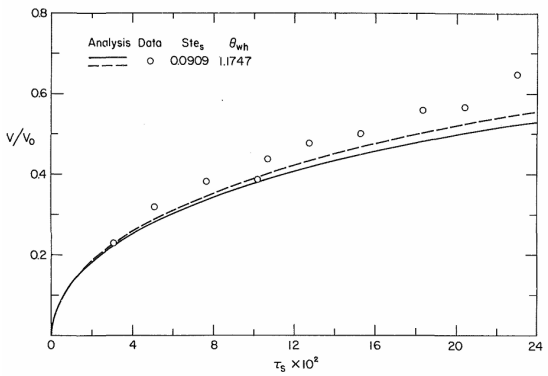
Figure 4.4: Comparison of simulated liquid fraction contours at 1, 2, 3, and 6 min with the experimental melting front evolution reported by Gau and Viskanta.

4.1.2 Validation of Liquid Fraction Prediction

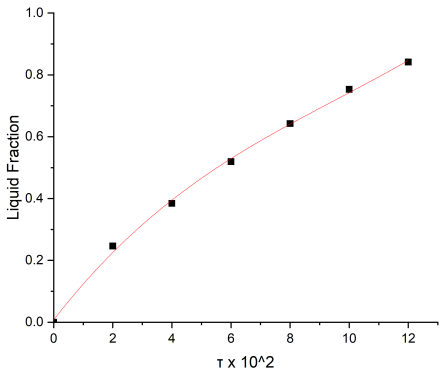
The numerical model is validated by a comparison of the predicted evolution of liquid fraction with experimental results reported by Gau and Viskanta for the melting of gallium. The comparison was done in terms of the dimensionless time parameter, τ, to be consistent with the experimental representation. The predicted liquid fraction from the present simulation is compared with the experimental measurements reported by Gau and Viskanta in Figure 4.5. In the experimental plot, the measured melted volume fraction V/V_0 is shown as circular symbols and the predicted liquid fraction from the enthalpy-porosity model is shown as a numerical result.

The numerical results are in good agreement with the experimental melting trend. The predicted liquid fraction increases continuously with the dimensionless time, showing the same behaviour observed in the experimental measurements. The results show that during the early stage of melting, the liquid fraction increases gradually, which indicates that the phase change is dominated by heat conduction through the solid PCM. With melting, the liquid fraction growth rate increases because the liquid region expands and the buoyancy-driven flow becomes more important.

The numerical prediction agrees well with the experimental data in the first stage, showing a similar melting progression (see Figure 4.5). The simulation results show a small higher liquid fraction compared to the experimental values during the progression of the melting process. The simulation predicts liquid fraction of ~ 0.64 at $\tau \approx 8$ while the experimental measurement is ~ 0.50. For the last comparison point, at $\tau \approx 12$, the numerical model predicts a liquid fraction of about 0.84 , compared to an experimental melted volume fraction of about 0.65.



(a)Experimental data and prediction analysis from Gau and Viskanta [107] [Source]



(b)Simulation results of gallium melting

Figure 4.5: Comparison between experimental data of liquid fraction and simulation results

The higher melting rate predicted by the numerical model can be related to the differences between the numerical assumptions and the experimental conditions . In the simulation, the thermophysical properties of the PCM were considered to be constant during the entire melting process. In the experimental system, properties such as thermal conductivity, density and viscosity are temperature-dependent, affecting heat transfer and the development of natural convection during melting.

The faster melting prediction could also be a result of the boundary conditions used in the numerical model. The heated wall was modeled as an ideal constant temperature boundary condition, enabling continuous heat transfer into the PCM. In the experimental set-up, heat losses from the container and potential thermal resistance between the heating source to the PCM may reduce the actual heat supplied to the material. These effects are not considered in the numerical model and could result in a lower experimental melting rate.

The difference between the numerical and experimental results can also be attributed to the method used to determine the melted fraction. The Gau and Viskanta experimental values were based on the visual observation of the melting interface, while the numerical liquid fraction was obtained from the local enthalpy balance inside each computational cell . The numerical method gives a continuous distribution of the liquid fraction in the domain. Experimental measurements can have uncertainties in the transition region between the solid and liquid phases.

The numerical model is able to reproduce the main characteristics of the experimental melting behaviour despite the difference in melting rate. The predicted liquid fraction exhibits the same increasing trend and captures the acceleration of melting due to the transition from conduction-dominated heat transfer to convection-assisted melting.

Chapter 5

Results

5.1 Melting Behavior of RT18 PCM

The melting behavior of RT18 PCM was studied by monitoring the evolution of the liquid fraction during the transient simulation. The liquid fraction correspond to the amount of PCM that has changed phase from solid to liquid, with 0 representing a completely solid phase and 1 a completely molten region. The phase transition process was studied at different simulation times to investigate the movement of solid–liquid interface and the effect of heat transfer mechanisms within the PCM domain.

In the beginning of the simulation, the heat transfer is mainly conduction from the heated boundary to the PCM. Melting was initiated in the vicinity of the heated wall, where a thin high liquid fraction region was created, as shown in Figure 5.1. The values of the liquid fraction were near zero, which means that most of the PCM was still solid. In this early stage, the melting front was rather uniform because the energy transfer process was dominated by heat conduction before significant liquid motion occurred.

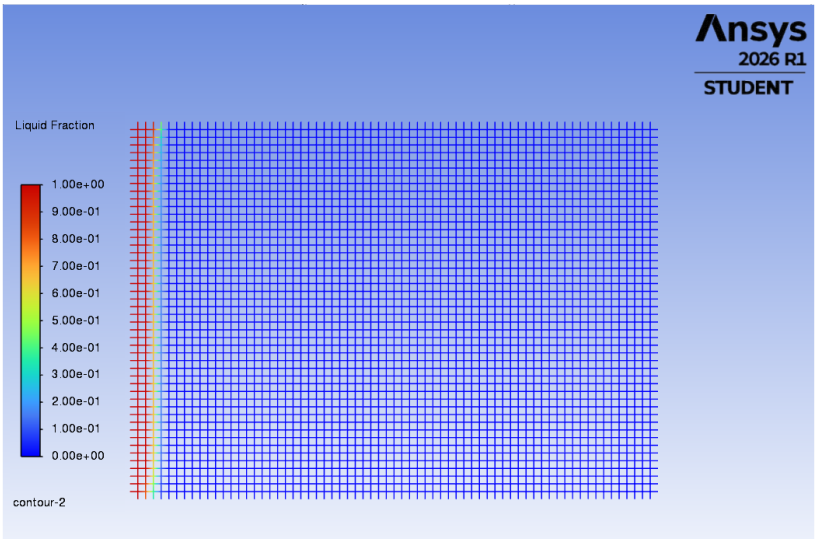


Figure 5.1: Liquid fraction distribution of RT18 PCM after 60 s.

The temperature distribution at 180 s and 300 s is shown in Figures 5.2 and 5.3, respectively. The melted region continued to grow away from the heated boundary. The increase in liquid fraction was gradual indicating the continuous absorption of thermal energy by PCM. In the early stage, the melting interface was relatively close to the vertical direction, which indicated that conduction was still the dominant heat

transfer mechanism. In the zone adjacent to the heated wall the liquid fraction values were larger, whereas the major part of the PCM volume was in the solid state.

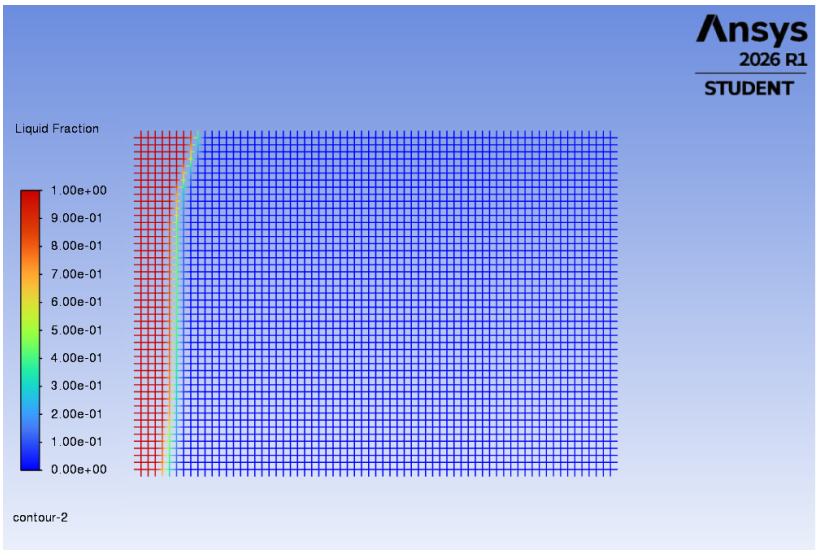


Figure 5.2: Liquid fraction distribution of RT18 PCM after 180 s.

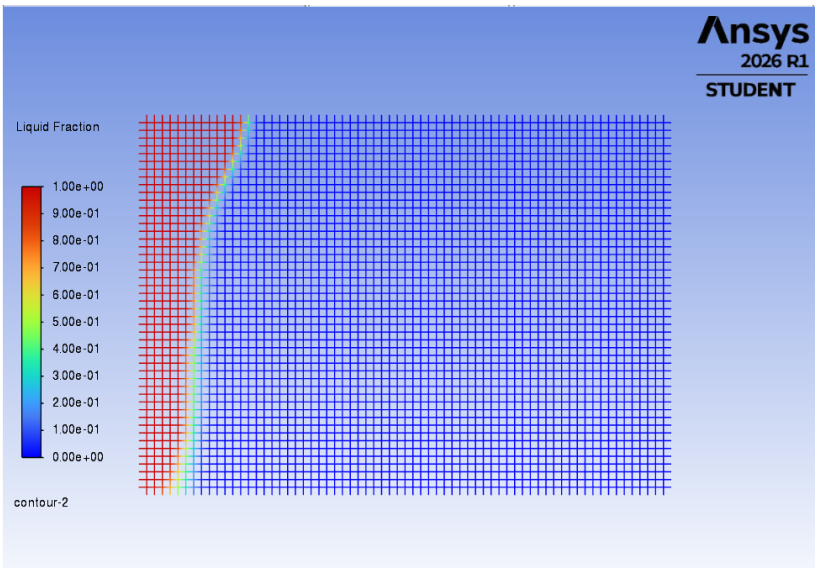


Figure 5.3: Liquid fraction distribution of RT18 PCM after 300 s.

Figure 5.4 shows a significant change in the shape of the melting interface after 420 s. The liquid region was wider in the upper part of the PCM domain than in the lower part. This behaviour indicates the increasing role of natural convection in the melted PCM. Then, as soon as enough liquid PCM was formed, the density differences due to the temperature variation generated buoyancy driven flow. The warmer liquid PCM moved upward, increasing the heat transport in the upper part, and a non-uniform melting pattern was produced.

Convection effects became more important at longer simulation times. From Figure 5.5 it is seen that a large part of PCM has melted and become liquid and only a smaller solid region is left at the unheated side

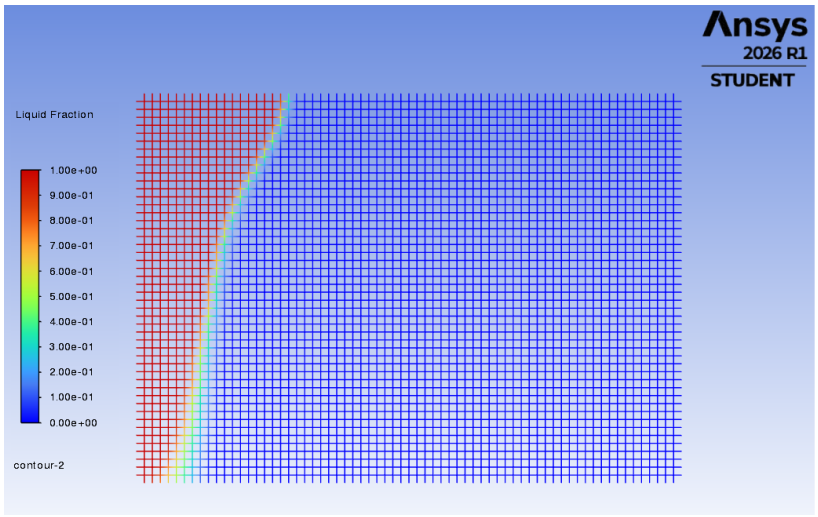


Figure 5.4: Liquid fraction distribution of RT18 PCM after 420 s.

of the enclosure. The curvature of the melting interface indicates that heat transfer was no longer dominated by conduction. The buoyancy-driven flow of the molten PCM enhanced the thermal transport and hastened the melting process in the regions with buoyancy-driven flow.

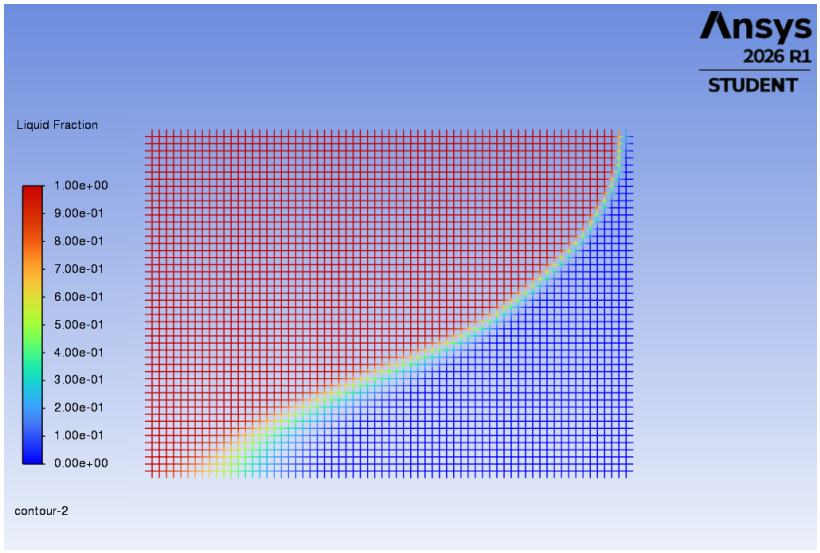


Figure 5.5: Liquid fraction distribution of RT18 PCM after 2010 s.

At the end of the simulation period (3600 s) the RT18 PCM was almost completely melted as shown in Figure 5.6. The liquid fraction was close to one over almost the entire computational domain, which indicated that the PCM absorbed enough energy for completing the phase transition. Near the final melting boundary, a small region of smaller liquid fraction still remains, suggesting that more time is required to fully melt.

The melting process of RT18 PCM can be divided into two steps. During the first stage, heat transfer was primarily due to conduction and melting occurred gradually near the heated surface. As the liquid layer grew, natural convection became more important and altered the shape of the melting front. The results show that the enthalpy-porosity model captures the transition from conduction-dominated melting

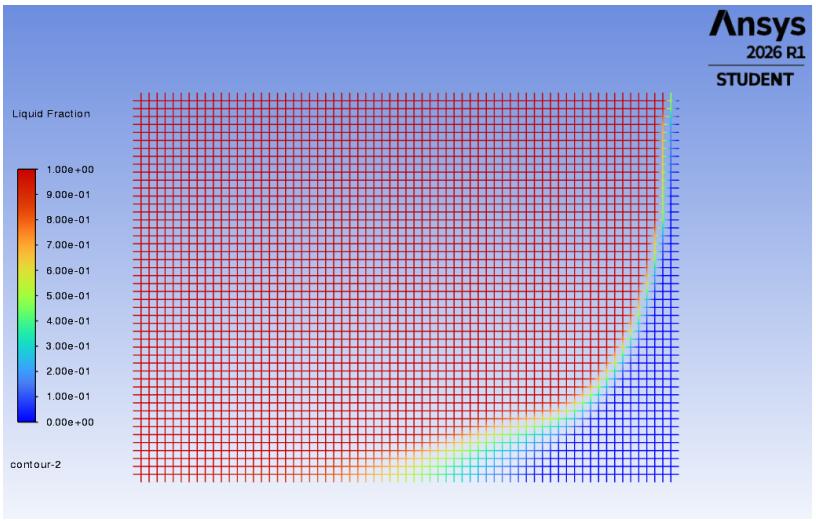


Figure 5.6: Liquid fraction distribution of RT18 PCM after 3600 s.

to convection-enhanced melting correctly. The observed melting pattern is consistent with the expected one for PCM systems ([104] [108]), where the heat transfer is more and more affected by the motion of the fluid when enough liquid is formed.

5.2 Temperature Distribution During RT18 PCM Melting

The temperature evolution of the RT18 PCM domain during the melting process was studied to understand the heat transfer behavior and thermal response of the storage unit. The temperature contours at different simulation times are shown in Figures 5.7–5.12. The temperature profile provides information about the heat propagation from the heated boundary into the PCM and its relation to the development of the melting front.

At the beginning of the simulation, the temperature increase was initially localized near the heated wall (see Figure 5.7). A large temperature gradient was observed between the heated region and the rest of the solid PCM. The temperature around the heat source was about 309 K while the far regions were close to the initial temperature of the PCM. Thus, in the early melting stage, the heat transfer was dominated mostly by conduction, where thermal energy transferred slowly through the solid PCM.

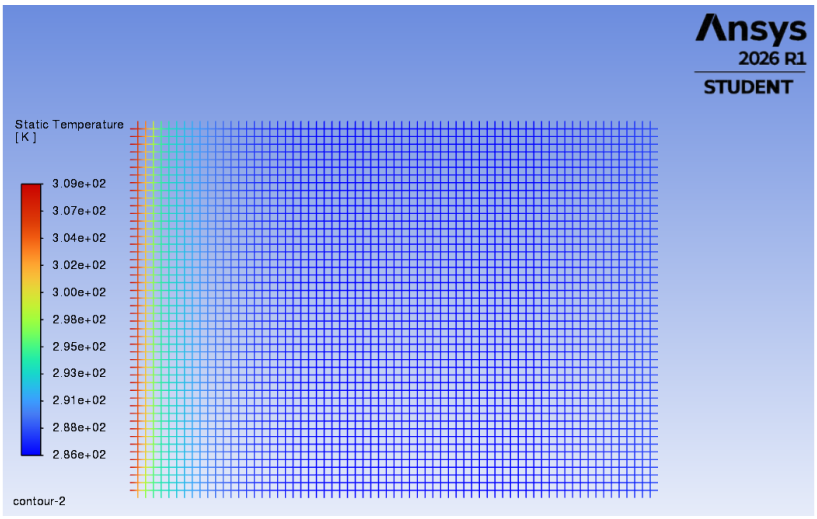


Figure 5.7: Temperature distribution of RT18 PCM after 60 s.

With increasing the heating period the thermal field extended more into the PCM domain. As seen in Figures 5.8 and 5.9, the high temperature region near the heated boundary continued to grow and the temperature gradient became less concentrated. The increase in temperature is due to the PCM absorbing sensible heat before and during the phase change. In the vicinity of the heated surface the temperatures were above the melting range of RT18, therefore a liquid layer was formed the thickness of which increased with time.

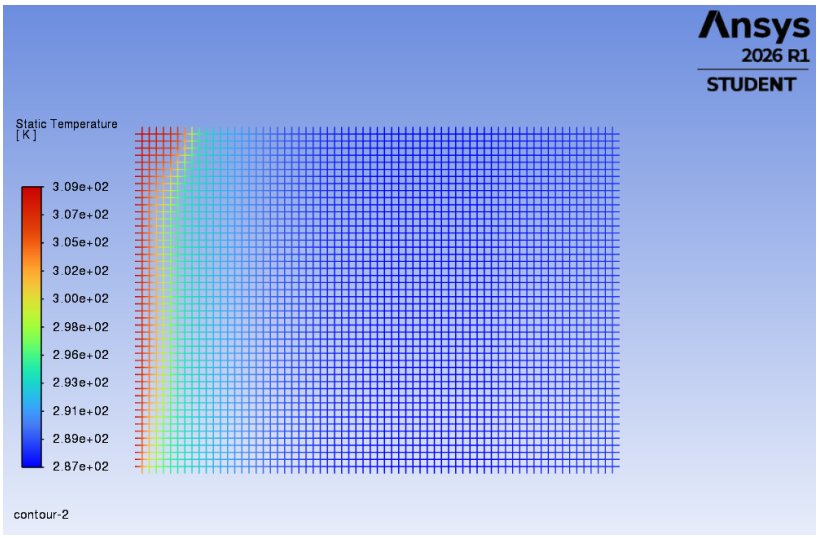


Figure 5.8: Temperature distribution of RT18 PCM after 180 s.

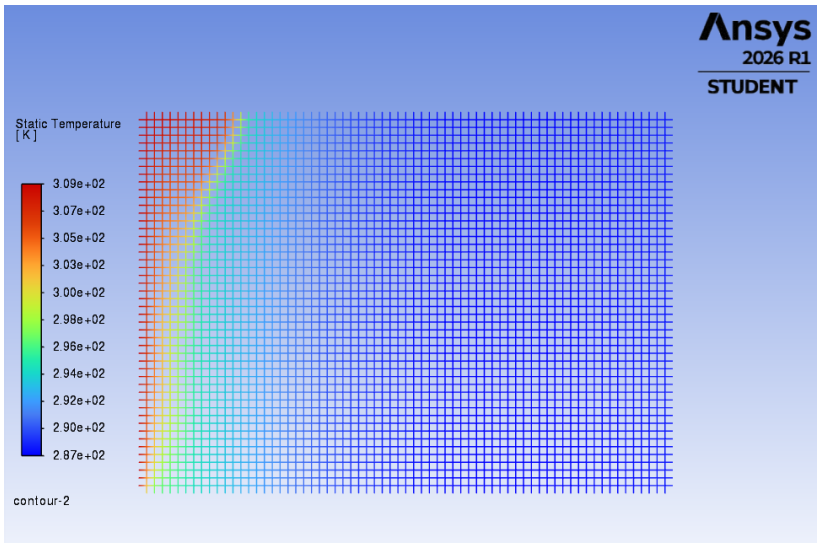


Figure 5.9: Temperature distribution of RT18 PCM after 300 s.

As shown in Figure 5.10, the temperature field showed a distinct change in distribution at 420 s. The development of liquid PCM and the onset of buoyancy driven flow caused the temperature contours to become less uniform. The warmer liquid phase adjacent to the heated wall moved upward carrying thermal energy to the upper portion of the enclosure. This resulted in the formation of a higher temperature zone in the upper region of the PCM domain as compared to the lower region. The change in the temperature distribution corresponds to the curved melting interface shown in the contours of the liquid fraction.

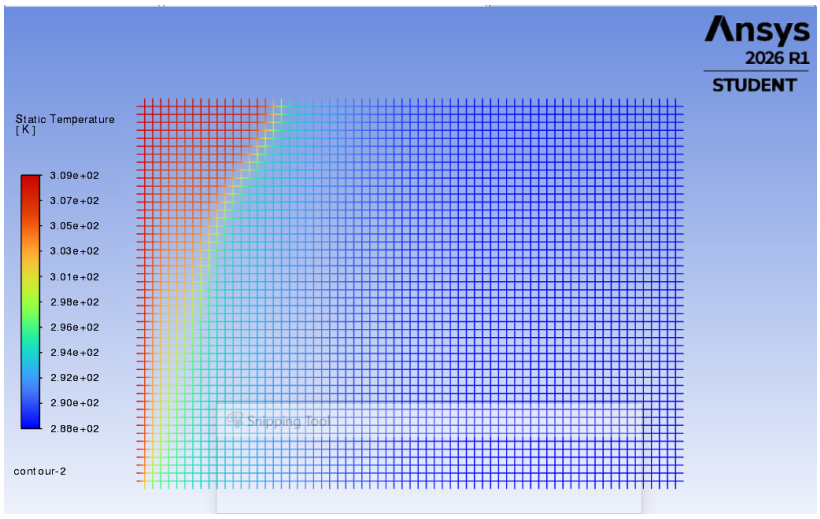


Figure 5.10: Temperature distribution of RT18 PCM after 420 s.

By the 2010 s, a larger portion of the PCM domain had temperatures near the melting range (Figure 5.11). The upper region was hotter due to natural convection, and the rest of the cooler region was located by the unheated side of the enclosure.

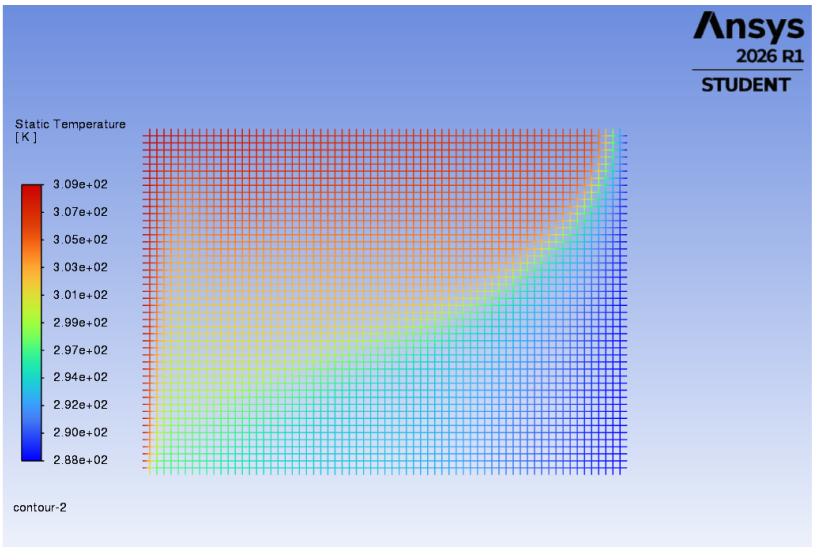


Figure 5.11: Temperature distribution of RT18 PCM after 2010 s.

At the end of the simulation period (after 3600 s) the temperature distribution became more uniform throughout the PCM domain as shown in Figure 5.12. The thermal equilibrium was close, as most of the PCM approached the heated wall temperature. The decrease in temperature gradients indicated that the majority of the thermal energy was absorbed by the PCM and that the melting process was almost complete. The residual temperature difference in the domain was attributed to the last phase transition where the last solid regions required more energy to be completely melted.

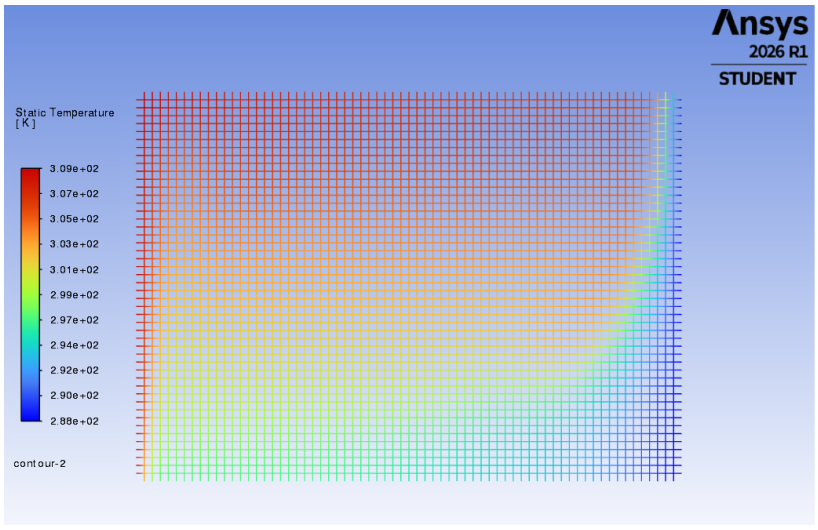


Figure 5.12: Temperature distribution of RT18 PCM after 3600 s.

The temperature contours show the heat transfer development during RT18 PCM melting. The temperature evolution is consistent with the liquid fraction results confirming that the enthalpy-porosity model was able to accurately capture the transient thermal behavior of the PCM during the phase change.

5.3 3D Cold Storage Melting Behavior

The cooling behavior of the RT5 PCM system was studied by considering the temperature evolution of air and PCM as well as the variation of liquid fraction during the transient cooling process. Initial temperature of PCM was 277.5 K and it was in a fully solid state and temperature of air inside the closed enclosure was 298 K. The temperature difference between air and PCM produced a heat transfer process in which thermal energy was transferred from the warmer air to the colder PCM. The absorbed thermal energy resulted in melting of the PCM and hence increase in liquid fraction.

Figure 5.13 shows the average liquid fraction of RT5 PCM as a function of simulation time. At the beginning of the cooling process, the liquid fraction increases slowly from zero when heat is transferred from the surrounding air to the PCM. The first increase is relatively slow as the PCM first needs to increase in temperature from its initial temperature before significant melting occurs. Heat transfer in this period is dominated by sensible heating of the PCM.

As the temperature of the PCM reaches its melting range, more and more of the absorbed thermal energy is used for the process of phase transition. The liquid fraction increases steadily throughout the simulation, reaching about 0.20 at 650 s. The continuous growth of the liquid fraction indicates the PCM is absorbing heat from the ambient air using latent heat storage. The low final liquid fraction indicates that a large part of the PCM is still in the solid state during the period studied, so the storage system is able to take in additional thermal energy after the simulation time.

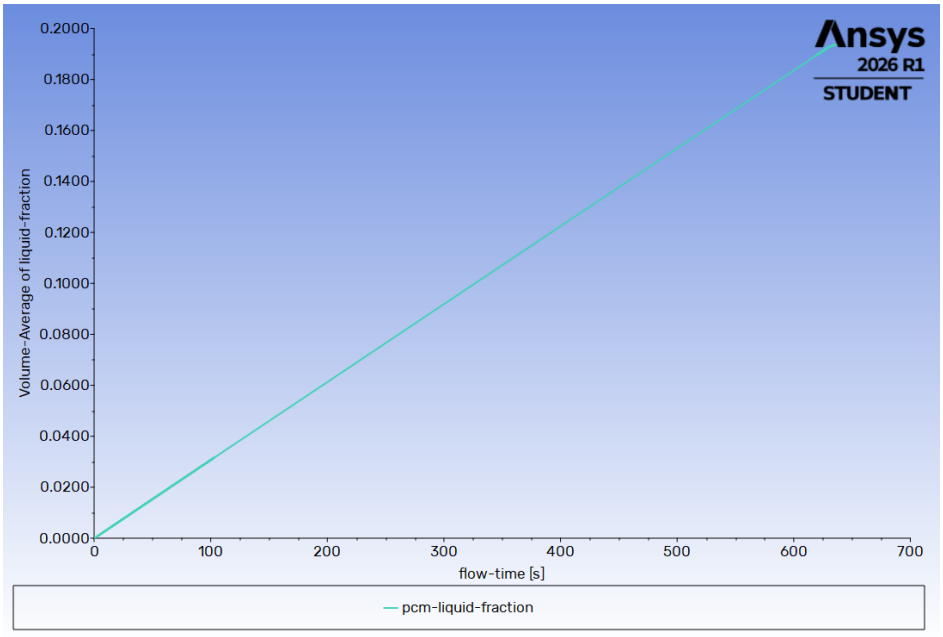


Figure 5.13: Average liquid fraction evolution of RT5 PCM during the cooling process.

The temperature response of the PCM is shown in Figure 5.14. The average temperature of PCM increases slowly from roughly 277.5 K to 277.6 K during the simulation time. The small temperature variation is linked to the latent heat uptake process of the PCM. As the phase change temperature of the PCM is approached, the absorbed heat from the air is mostly used to melt the PCM, not to raise the PCM temperature. This behavior allows the PCM to absorb heat from the surrounding air while maintaining a relatively stable temperature.

Figure 5.15 shows the effect of the PCM cooling on the air inside it. During the first stage of the simulation, the air temperature decreases rapidly from about 298 to 280 within the first 100 s. This fast reduction of

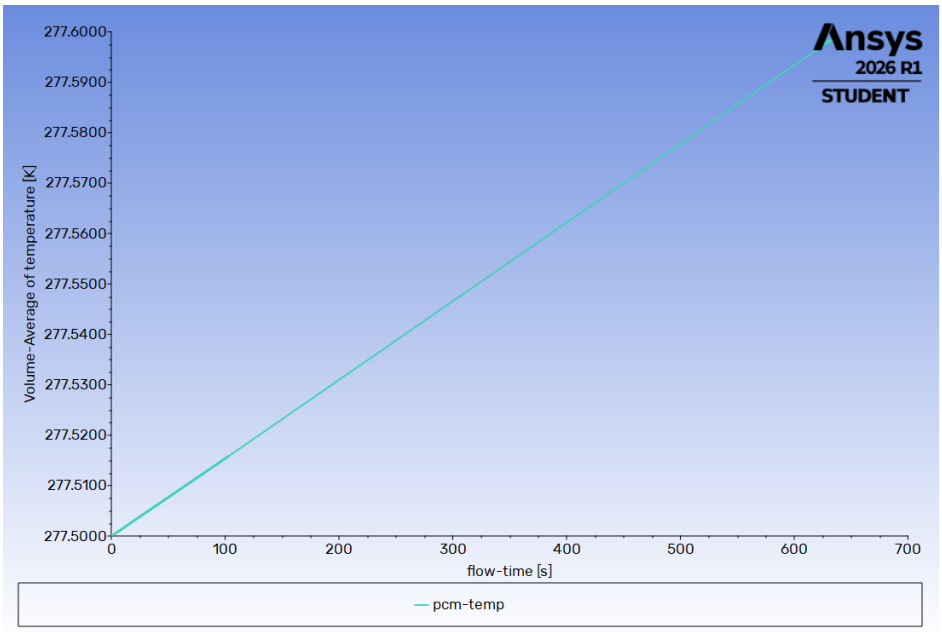


Figure 5.14: Average temperature evolution of RT5 PCM during cooling.

temperature is because at the beginning the temperature difference between the warm air and the cold PCM is high and the heat transfer rate is higher. The reduction of the driving temperature difference between the two regions causes the reduction of the temperature reduction rate as the air temperature approaches the PCM melting temperature.

After about 100 s the air temperature is still decreasing but with a reduced rate and about 279 K at the end of the simulation. The decrease in cooling rate implies that the system is moving toward a thermal equilibrium condition, where the rate of heat transfer from the air to the PCM is decreasing. The temperature behavior shows the capability of RT5 PCM to reduce the air temperature without the use of active refrigeration, since the stored latent heat capacity continues to cool down during the simulation period.

Figure 5.16 presents the spatial distribution of liquid fraction inside the PCM domain. The contour presents that the melting is not homogenous in all the volume of PCM. The liquid fraction is higher in the regions closer to the air-PCM interface, since these regions are directly heated by the warmer air. Inside, the PCM has a lower liquid fraction since heat needs to be transmitted thru the layer of the previously melted PCM to reach the deeper zones.

The non-uniform melting pattern is due to the heat transfer mechanism within the closed enclosure. Heat transfer is by natural convection in air and conduction through the PCM, since the flow is stagnant. The warmer air in the upper region of the enclosure transfers heat to the surface of the PCM and cooler air moves downward because of the density differences. This leads to a non-uniform heat transfer rate over the PCM surface and therefore different melting rates in the storage volume.

The results show that the RT5 PCM can effectively reduce the temperature of the trapped air by absorbing thermal energy through phase transition. The increase in liquid fraction shows the thermal energy storage in PCM and the decrease in air temperature shows the cooling capacity of the system. The capability to control temperature and store latent heat makes PCM based cooling systems suitable for applications where continuous refrigeration power is unavailable such as rural cold storage to reduce post-harvest losses.

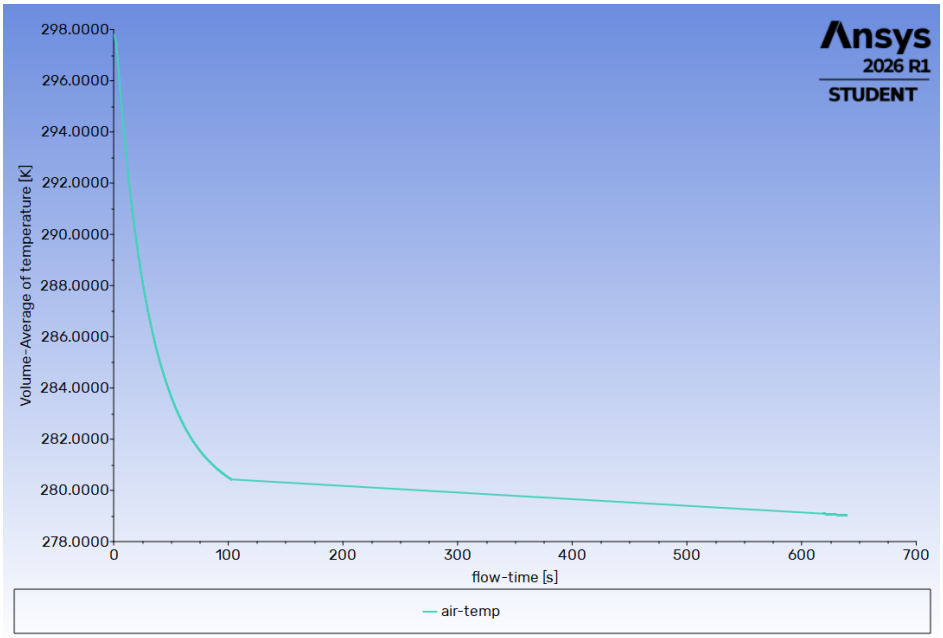


Figure 5.15: Air temperature variation during PCM-assisted cooling.

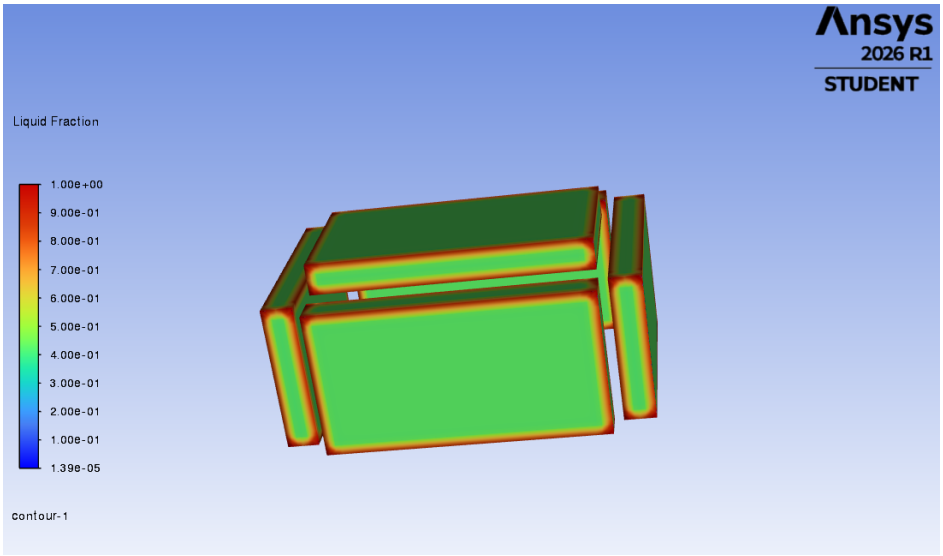


Figure 5.16: Three-dimensional liquid fraction distribution of RT5 PCM during cooling.

Chapter 6

Discussion

6.1 Thermal Behaviour of PCM During Phase Transition

The numerical study demonstrated that phase change materials (PCMs) are capable of passive cooling thru adsorption of latent heat. For the cold storage application, RT5 PCM was initially in the solid state at 277.5 K and the ambient air inside the insulated enclosure was initialized at 298 K . The temperature difference between air and PCM created a thermal gradient that favored heat transfer from warmer air to colder PCM. Therefore the PCM absorbed the thermal energy and gradually melted, as can be seen from the increase of the liquid fraction.

The change of the liquid fraction indicates that the melting process was a gradual one, not an abrupt one. During the first stage of melting the liquid fraction grew relatively slowly as the absorbed heat was first utilized to raise the temperature of the solid PCM. So sensible heat transfer dominated prior to the PCM entering the melting temperature range. This behavior is consistent with the basic rule of latent heat storage, where the temperature of the PCM increases at first until the melting point is reached. The main part of the absorbed thermal energy is later used for the solid–liquid phase transition instead of the increase of the temperature of the PCM.

When the melting temperature range was achieved, the liquid fraction increased continuously and reached about 0.20 at 650 s. The small liquid fraction attained at the end of the simulation demonstrates that only a fraction of the PCM was melted during the considered time frame. As a consequence, a large latent heat storage capacity was available. This type of behavior is advantageous in cold storage applications as the PCM can take in extra heat entering the storage system before fully melting.

The temperature response of the PCM also supports the latent heat storage mechanism. The average PCM temperature increased only slightly from about 277.5 K to 277.6 K during the simulation period. The narrow range of temperature indicates that PCM absorbed energy mainly by phase change instead of sensible heating. One of the major advantages of PCM based thermal storage systems is the almost constant temperature during phase change especially for applications where temperature regulation is required.

6.2 Cooling Performance of RT5 PCM

The cooling performance of the PCM was measured by the temperature drop of the enclosed air. The air temperature dropped dramatically from about 298 K to 280 K in the first 100 s. This rapid decrease was attributed to the large initial temperature difference between air and PCM that created a high driving force for heat transfer.

As the air temperature decreased and neared the PCM temperature, the temperature gradient reduced

and thus the cooling rate gradually decreased. This behavior suggests that the system is close to thermal equilibrium during the simulation. Initially, the large temperature difference between the PCM surface and air dominated the heat transfer. But with the decrease of the temperature difference, the heat transfer rate also decreased correspondingly.

The final air temperature of 279 K indicates that RT5 PCM can provide a cold environment without any active refrigeration. PCM based systems differ from conventional refrigeration systems, in which the heat is removed continuously and act as thermal buffers, which absorb the heat thru latent heat storage. The remaining fraction of solid PCM at the end of the simulation shows that there was still available cooling capacity.

6.3 Analysis of Melting Distribution and Heat Transfer Mechanisms

The liquid fraction distribution revealed that the melting was not uniform in the entire PCM domain. Higher liquid fractions were observed near the air-PCM interface, while the regions deeper into the PCM were predominantly solid. The observed behavior is explained by the need of heat to penetrate thru the melted PCM layer before reaching the inner solid PCM region.

The non-uniform melting behavior emphasizes the importance of thermal resistance during PCM phase transition. However, many organic PCMs have relatively low thermal conductivity, which limits the heat penetration and increases the melting and solidification time, despite the high energy storage density of PCMs.

In the present study, the air inside the enclosure was assumed stagnant, so that heat transfer was by conduction within the PCM and natural convection within the air region. The temperature was not uniform throughout the air, and this produced density differences and buoyancy driven movement. Thus, different melting behaviors and heat transfer rates in different regions of the PCM were observed.

The observed melting behavior emphasizes the need for CFD modeling in PCM systems. Simple conductive models cannot describe the coupling of phase change, temperature distribution and buoyancy driven flow. Therefore numerical modeling helps to better understand the PCM behavior in thermal storage applications.

6.4 Comparison Between RT5 Cooling Performance and PCM Selection Criteria

The choice of a PCM for cold storage applications is based on several thermophysical properties including melting temperature, latent heat capacity, thermal conductivity, chemical stability and compatibility with the intended application.

RT5 PCM was chosen due to its melting temperature range, which is suitable for low temperature thermal energy storage applications. The simulation results show that RT5 can effectively lower the temperature of the storage environment, with the temperature close to the phase transition range.

But the simulation also shows a limitation of the PCM thermal conductivity. The interior regions are melting at a slow rate indicating the limited heat transfer in the PCM. But this limitation allows a long cooling duration but reduces the rate of thermal energy absorption of the PCM.

To overcome this limitation, techniques to enhance heat transfer can be considered such as:

- use of metallic fins to increase the heat transfer area,
- addition of high conductive materials such as graphite,

- optimization of PCM thickness,
- modification of PCM arrangement inside the storage enclosure.

Such approaches may improve the heat distribution in the PCM and reduce the thermal resistance during a phase change.

6.5 Implications for Rural Cold Storage Applications in Ghana

The simulation results indicate that PCM-based cooling systems can be an alternative solution for rural cold storage applications where the supply of electricity is not reliable. Like traditional refrigeration systems, they depend on constant electrical energy and regular maintenance, which can be problematic in remote agricultural communities.

The RT5 PCM can decrease the air temperature from 298 K to about 279 K, showing its capability to maintain suitable storage conditions for temperature-sensitive agricultural products. This is especially important to reduce post-harvest losses of fruits and vegetables in areas where cold-chain infrastructure is still limited.

Storage systems based on PCM can also complement renewable energy technologies. Examples include, for instance, PCM units that can be charged with solar energy when solar availability is high and provide cooling during times of no electricity generation. This approach can enhance reliability and sustainability of decentralized cold storage systems.

However, for practical implementation, other factors such as PCM encapsulation, material cost, thermal cycling stability, leakage prevention and long-term performance under the tropical climatic conditions need to be taken into account.

6.6 Numerical Modelling Considerations and Limitations

The accuracy of the PCM simulation strongly depends on the assumptions and numerical parameters that are used in the model. The phase transition behavior was described using the enthalpy-porosity method in this work. In this approach the liquid fraction is employed as an indicator of the phase state of the PCM and the mushy region is treated as a porous medium.

A mesh independence study was performed with mesh sizes of 1.5 mm and 1.3 mm. The results demonstrated similar trends in the evolution of liquid fraction and temperature, indicating that further mesh refinement produced negligible effects. Therefore, the selected mesh resolution was considered appropriate to capture the main thermal behavior of the system.

Although the behavior of PCM has been successfully predicted some limitations exist. The simulation assumes constant thermophysical properties, but the real properties of PCM such as density, viscosity and thermal conductivity are temperature dependent. Beside, practical effects such as heat losses, imperfect insulation, PCM expansion and degradation during repeated thermal cycling were not considered.

Future studies should include temperature dependent properties, experimental validation and long term cycling analysis for model accuracy.

6.7 Design Optimization Considerations

However, while the present study demonstrates the feasibility of applying RT5 PCM for passive cooling, further optimization is required to enhance system performance.

The disadvantage of the present configuration is the relatively low thermal conductivity of the PCM that limits the heat transfer to the inner regions. Therefore, future design improvements should focus on decreasing the thermal resistance and improving the heat transfer.

Possible optimization strategies include:

6.7.1 PCM Geometry Optimization

Reducing the thickness of PCM or increasing the ratio of surface area to volume can reduce the distance needed for heat conduction and increase melting.

6.7.2 Inclusion of Heat Transfer Enhancement Structures

Metallic fins or conductive structures can improve the heat distribution in the PCM and reduce the temperature gradients.

6.7.3 PCM Layout Optimization

The placement and orientation of PCM modules will affect the air flow pattern and heat transfer efficiency. Hence, the placement optimization of PCM can improve the overall cooling performance.

6.7.4 Comparison of PCM Material

Future work should compare different PCM materials in terms of cooling time, latent heat capacity, cost and suitability for the environmental conditions in Ghana.

Chapter 7

Conclusion and Future Work

7.1 Conclusion

Post-harvest losses are an ever-growing problem in the developing world, especially in rural areas where access to reliable power and traditional refrigeration systems is often unavailable, creating a demand for alternative cooling technologies. The present work investigated the application of phase change material (PCM) based thermal energy storage (TES) as a passive cooling solution for rural cold storage. A computational fluid dynamics (CFD) model was developed to assess the thermal behavior of an RT5 PCM system during the cooling process.

The numerical model was developed implementing the enthalpy-porosity method to describe the phase change behavior of the PCM. The model accounted for heat transfer between the PCM and the ambient air in a closed storage enclosure. The PCM was initially in the solid state at 277.5 K and the air temperature was kept at 298 K. The heat transfer was driven by the temperature difference between the two regions, which led to the absorption of thermal energy by the PCM and its gradual melting.

The numerical model was validated against the experimental data from the previous studies and the reliability was assessed by mesh independence analysis. The validation results showed that the model could reproduce the overall melting behavior and the evolution of the liquid fraction as observed experimentally. Although the numerical predictions showed some differences from the experimental measurements, mainly due to the assumptions of constant thermophysical properties and idealized boundary conditions, the model could still predict the major features of PCM phase change behavior.

The cooling performance of RT5 PCM system was evaluated by studying the reduction of the air temperature, the evolution of the temperature of PCM and the variation of liquid fraction. The results showed that the PCM was able to reduce the air temperature inside the storage enclosure from about 298 K to 279 K during the whole simulated period. The large temperature difference between the warm air and the cold PCM was responsible for the rapid temperature reduction in the initial stage. As the system approached thermal equilibrium the cooling rate decreased due to the decrease of the temperature difference.

The temperature of the PCM was almost constant during the cooling process. It increased slightly from about 277.5 K to 277.6 K. This behavior confirms the role of latent heat storage, where most of the thermal energy absorbed was used for phase change, not for increasing the PCM temperature. The increase of liquid fraction during the whole simulation also confirmed the PCM absorbed heat from the environment around thru melting.

The liquid fraction distribution showed that melting was not uniform in the PCM domain. Higher liquid fractions were observed in the regions near the air-PCM interface due to direct heat transfer from the surrounding air, whereas the inner regions remained mostly solid due to the thermal resistance of the PCM layer. This behavior emphasizes the necessity of heat transfer enhancement techniques to improve PCM

performance.

The results of this study indicate that RT5 PCM has great potential to be applied in passive cold storage systems. The PCM can absorb thermal energy while keeping a relatively stable temperature, which makes it suitable for protecting temperature-sensitive agricultural products during storage. The results also show that PCM-based cooling systems could be an alternative solution to decrease the dependency on electrically driven refrigeration systems in rural areas.

However, the study also pointed out limitations of the thermal conductivity and heat transfer resistance of the PCM. The PCM has a high thermal storage capacity . However, the heat propagation into the interior regions is slow which limits the rate of phase transition. Thus, more improvements are needed before practical implementation, especially for applications requiring rapid cooling.

7.2 Future Work

Further research should focus on the enhancement of the thermal performance and practical applications of PCM-based cold storage systems. Studies on heat transfer enhancement techniques such as the use of metallic fins, conductive additives and optimized PCM geometries should be carried out to reduce the thermal resistance and improve melting uniformity.

Future studies should also evaluate other PCM materials with melting temperatures suitable for specific agricultural products in storage under Ghanaian climatic conditions. A comparison of PCMs based on cooling duration, thermal storage capacity, cost and long-term stability would provide useful information for the material selection.

It is also suggested to do experimental testing of the proposed storage system to validate the numerical predictions in real operation. Future models should take into account the temperature-dependent thermophysical properties, heat losses thru the storage walls and long-term thermal cycling effects to increase the prediction accuracy.

The integration of PCM cold storage systems with renewable energy sources, especially solar energy, should be investigated. Such systems can provide reliable cooling options for rural communities with limited access to grid electricity. Further studies on system design, economic analysis and field performance evaluation would assist in the development of PCM-based cold storage technologies to reduce post-harvest losses in Ghana and similar regions.

AI Declaration

I declare that a part of this work was done by the assistance of AI tools. These AI tools were specifically used to correct grammatical errors and spelling mistakes and to rephrase some part of the work for better representation.

Bibliography

[1] Central Intelligence Agency. The world factbook: Ghana country profile. https://worldfactbookarchive.org, 2026. Accessed: 2026-07-30. 1

[2] Ministry of Foreign Affairs and Regional Integration, Ghana. About ghana: Overview of geography and borders. https://mfa.gov.gh, 2026. Accessed: 2026-07-30. 1

[3] A. Amo-Aidoo, E.N. Kumi, O. Hensel, J.K. Korese, and B. Sturm. Solar energy policy implementation in ghana: A leap model analysis. *Scientific African*, 16:e01162, 2022. 1

[4] Ephraim Bonah Agyekum, Muhammad Amjad, Syed Aziz Shah, and Martin Nti Ansah. Promoting the solar industry in ghana through effective public–private partnership: A review. *Energies*, 15(1):17, 2021. 1

[5] 350 Ghana Reducing Our Carbon (350 GROC). Bridging Ghana's energy access gap: The role of decentralized renewable energy systems. 350 GROC Campaign Report Brief, 2025. 1

[6] Copenhagen Consensus Center. Ghana priorities: Rural electrification policy brief. Sector assessment report, Ghana Statistical Service & National Development Planning Commission, 2020. 1

[7] Isaac Adocta, Frank Owusu-Ansah, and Fuseini Yakubu. Understanding household energy decisions and biomass reliance in off-grid rural Ghana. *Journal of Sustainable Development and Fueling Homes via ScienceDirect*, 19(3):45–58, 2025. 1

[8] Michael Acheampong, Robert Osei-Kyei, and Albert Danso. Financing off-grid solar in rural Ghana: Overcoming capital barriers and the poverty premium. *Energy Policy*, 185:113942, 2024. 1

[9] Simon Bawakyillenuo and Ishmael Agbelie. Why rural households stay off the clean cooking grid: The mismatch between solar pv electrification and thermal energy needs in Ghana. *World Development Perspectives*, 31:100518, 2023. 1

[10] Ministry of Energy, Republic of Ghana. The national clean cooking strategy and lpg promotion framework: Integrated solutions for rural communities. Policy implementation roadmap, Ghana Energy Commission, 2025. 1

[11] Caleb Wright, Roger Sathre, and Shashi Buluswar. The global challenge of clean cooking systems. *Food Security*, 12(6):1219–1240, 2020. 1

[12] Kokouvi Edem N'TSOUKPOE, Sara Claude LEKOMBO, Francis KEMAUSUOR, Gaëlle Kafira KO, and El Hadji Bamba DIAW. Overview of solar thermal technology development and applications in west africa: Focus on hot water and its applications. *Scientific African*, 21:e01752, 2023. 1

[13] Vivien Kizilcec, Tash Perros, Iwona Bisaga, and Priti Parikh. Comparing adoption determinants of solar home systems, lpg and electric cooking for holistic energy services in sub-saharan africa. *Environmental Research Communications*, 4(7):072001, jul 2022. 1

[14] Baraka Kichonge and Samson Mwakapoma. Photovoltaic system performance in sub-saharan africa under environmental, technical and policy constraints. *Discover Sustainability*, 7(1):341, 2026. 1

[15] Barbara Mendecka, Giovanni Di Ilio, Vesselin K. Krastev, and Gino Bella. Technical assessment of phase change material thermal expansion for passive solar tracking in residential thermal energy storage applications. *Journal of Energy Storage*, 48:103990, 2022. 1

[16] Abraham Kribus and Michael Epstein. Chapter 2 - thermochemically regenerative flow batteries for solar electricity generation and storage. In Alejandro Datas, editor, *Ultra-High Temperature Thermal Energy Storage, Transfer and Conversion*, Woodhead Publishing Series in Energy, pages 35–56. Woodhead Publishing, 2021. 1

[17] Hossein Senobar, Abdul Wahab, Mojtaba Ahmadi, Omid Zabihi, Hans Kemper, Mark Easton, Minoo Naebe, and Hamid Khayyam. Phase change materials (pcms) for thermal energy storage systems. *Materials Today Sustainability*, 34:101369, 2026. 1

[18] Ahmed.H.N. Al-mudhafar, Mushtaq Talib Hamzah, and Ali Lateef Tarish. Potential of integrating pcms in residential building envelope to reduce cooling energy consumption. *Case Studies in Thermal Engineering*, 27:101360, 2021. 1

[19] Robert Geofrey, Eliaza Mkuna, Nyamsabhi M. Nyamwero, and Kulwa Mang'ana. Impact of postharvest handling technologies on income of tomato (solanum lycopersicum l.) smallholder farmers in mvomero, morogoro, tanzania. *African Journal of Science, Technology, Innovation and Development*, 17(1):65–79, 2025. 2

[20] Faizal Adams, Emmanuel Donkor, Jonathan Quaye, Anthony Adusei Jantuah, and Seth Etuah. Sustainable maize storage technology adoption in ghana: Implications for postharvest losses, farm income, and income inequality. *Food and Energy Security*, 13(5):e70011, 2024. e70011 FES3-2024-04-0102.R1. 2

[21] Moses Mosonsieyiri Kansanga, Kamaldeen Mohammed, Evans Batung, Sulemana Ansumah Saaka, and Isaac Luginaah. Lost harvest: examining the association between postharvest food loss and food insecurity in semi-arid ghana. *International Journal of Sustainable Development & World Ecology*, 30(7):776–791, 2023. 2

[22] Rahul Kumar, Amit Kumar Thakur, Lovi Raj Gupta, Anita Gehlot, and Vineet Singh Sikarwar. Advances in phase changing materials in solar thermal energy storage and applications, 9 2023. 2, 5, 6, 7

[23] Jianquan Lin, Qian Zhao, Haotian Huang, Hongzhi Mao, Yexin Liu, and Yimin Xiao. Applications of low-temperature thermochemical energy storage systems for salt hydrates based on material classification: A review. *Solar Energy*, 214:149–178, 2021. 2

[24] Kavati Venkateswarlu and S. V. Kota Reddy. Recent trends on energy-efficient solar dryers for food and agricultural products drying: a review. *Waste Disposal & Sustainable Energy*, 6(3):335–353, 2024. 2

[25] Abubakar Ibrahim Suleiman, Chan Hwang See, Firdaus Muhammad-Sukki, Ramasamy Mahendiran, Senthilarasu Sundaram, Mohamad Abidin, and Mohd Kamarudin. Deploying agrivoltaics in sub-saharan africa—a sustainable pathway toward energy-food security-challenges and opportunities: A review. *IEEE Access*, 13:87810–87833, 01 2025. 2

[26] Custodio Matavel, Harry Hoffmann, Constance Rybak, Stefan Sieber, Klaus Müller, Michael Brüntrup, and João Salavessa. Passive solar dryers as sustainable alternatives for drying agricultural produce in sub-saharan africa: advances and challenges. *Discover Sustainability*, 2(1):40, 2021. 2

[27] Flavio Odoi-Yorke, Richard Opoku, Charles K.K. Sekyere, and Francis Boafo Effah. Phase change materials for cold energy storage: Insights from three decades of research trends, advancements, and future directions. *Energy Exploration & Exploitation*, 44(3):1732–1783, 2026. 2

[28] Waseem Amjad, Anjum Munir, Fatima Akram, Aditya Parmar, Marcelo Precoppe, Furqan Asghar, and Faisal Mahmood. Decentralized solar-powered cooling systems for fresh fruit and vegetables to reduce post-harvest losses in developing regions: A review, 6 2023. 2

[29] Moses Mosonsieyiri Kansanga, Kamaldeen Mohammed, Evans Batung, Sulemana Ansumah Saaka, and Isaac Luginaah. Lost harvest: examining the association between postharvest food loss and food insecurity in semi-arid ghana. *International Journal of Sustainable Development & World Ecology*, 30:776–791, 04 2023. 3

[30] Waseem Amjad, Anjum Munir, Fatima Akram, Aditya Parmar, Marcelo Precoppe, Furqan Asghar, and Faisal Mahmood. Decentralized solar-powered cooling systems for fresh fruit and vegetables to reduce post-harvest losses in developing regions: a review. *Clean Energy*, 7:635–653, 05 2023. 3, 4, 5

[31] Edna Makule, Noel Dimoso, and S.A. Tassou. Precooling and cold storage methods for fruits and vegetables in sub-saharan africa—a review. *Horticulturae*, 8:776–776, 08 2022. 3

[32] Gloria Essilfie, Rosalyne Naa Norkor Baddoo, and S. Ayibor. Postharvest handling of indigenous vegetables in ghana: implications for reducing food loss and enhancing nutrition. *Frontiers in Horticulture*, 4, 09 2025. 3

[33] K. Senthil Kumar, R. Vasanthi, Mustafa Shakir, Arunkumar Munimathan, A.S. Manirathnam, Mohammad Mahtab Alam, Parvathy Rajendran, and It Ee Lee. Experimental investigation to enhancing the energy efficiency of a solar-powered visi cooler. *Scientific Reports*, 15:18327–18327, 05 2025. 3

[34] Jason Woods, Allison Mahvi, Anurag Goyal, Eric Kozubal, Adewale Odukomaiya, and Roderick Jackson. Rate capability and ragone plots for phase change thermal energy storage. *Nature Energy*, 6:295–302, 02 2021. 3, 4

[35] Michele De Angelo, Pamela Fabio, Grilletto Arcangelo, Cilenti Claudio, and Aprea Ciro. Achieving off-grid refrigeration in remote areas: A solar-powered vapor compression refrigerator prototype with pcm integration. *International Journal of Refrigeration*, 169:267–278, 10 2024. 3

[36] Adhiyaman Ilangovan, Samia Hamdane, Pedro Dinho da Silva, Pedro Dinis Gaspar, and Luís C. Pires. Promising and potential applications of phase change materials in the cold chain: A systematic review. *Energies*, 15:7683–7683, 10 2022. 3

[37] Gianluca Slaviero, Claudio Zilio, Marco Noro, Dario Traverso, Franco Traverso, and Simone Mancin. Feasibility study of potential application of off-grid cold room with ltes for food preservation in remote areas of africa. *Journal of Energy Storage*, 118:116237–116237, 03 2025. 3

[38] Babu Natarajan, Aravind Chellachi Kathiresan, and Senthil Kumar Subramanium. Development and performance evaluation of a hybrid portable solar cold storage system for the preservation of vegetables and fruits in remote areas. *Journal of Energy Storage*, 72:108292–108292, 07 2023. 3

[39] Michele Calati, Kamel Hooman, and Simone Mancin. Thermal storage based on phase change materials (pcms) for refrigerated transport and distribution applications along the cold chain: A review. *International Journal of Thermofluids*, 16:100224–100224, 10 2022. 3

[40] Raju R. Yenare, Chandrakant Sonawane, Kamal Sharma, Md Irfanul Haque Siddiqui, Dan Dobrotă, Choon Kit Chan, and Hitesh Panchal. Numerical analysis of phase change material placement and temperature effects in cold storage systems. *Alexandria Engineering Journal*, 129:1024–1038, 08 2025. 3, 4

[41] Maryam Hemmat, Kyle Teather, Kamran Siddiqui, and Anthony G. Straatman. An investigation into computational modelling of phase change materials using the enthalpy-porosity approach. *International Journal of Numerical Methods for Heat &amp Fluid Flow*, 35:1610–1641, 05 2025. 3

[42] Christoph Reichl, Svenja Both, Philipp Mascherbauer, and Johann Emhofer. Comparison of two cfd approaches using constant and temperature dependent heat capacities during the phase transition in pcms with experimental and analytical results. *Processes*, 10:302–302, 02 2022. 3

[43] Rejane De Césaro Oliveski, Fábio Becker, Luíz Alberto Oliveira Rocha, Cesare Biserni, and Gabriel Eduardo Strohm Eberhardt. Design of fin structures for phase change material (pcm) melting process in rectangular cavities. *Journal of Energy Storage*, 35:102337–102337, 01 2021. 3

[44] Adeel Arshad, Mohammed Ibrahim Alabdullatif, Mark Jabbal, and Yuying Yan. Towards the thermal management of electronic devices: A parametric investigation of finned heat sink filled with pcm. *International Communications in Heat and Mass Transfer*, 129:105643–105643, 10 2021. 4

[45] Robbie Crosby, Dudul Das, and Manosh C. Paul. Numerical study and experimental validation of a porous biochar supported form stable composite for thermal energy storage. *ENLIGHTEN (Jurnal Bimbingan dan Konseling Islam)*, 99:113314–113314, 08 2024. 4

[46] Ahmed Saad Soliman, Ahmed A. Sultan, and Mohamed A. Sultan. Effect of mushy zone parameter on phase change behavior of different configurations storage unit: Numerical simulation and experimental validation. *Sustainability*, 14(21), 2022. 4

[47] Farhan Lafta Rashid, Abbas Fadhil Khalaf, Asad Alizadeh, Mudhar A. Al-Obaidi, Soheil Salahshour, and Choon Kit Chan. Numerical investigation of the effect of the number of fins on the phase-change material melting inside a shell-and-tube cylindrical thermal energy storage. *Case Studies in Thermal Engineering*, 60:104754–104754, 06 2024. 4

[48] Rahul Joshi, Basant Singh Sikarwar, and Pushpendra Kumar Singh Rathore. Dual phase change material segmentation and orientation effects in shell-and-tube latent heat storage: A validated cfd simulation. *Energy Technology*, 14, 11 2025. 4

[49] Tianyu Yang, William P. King, and Nenad Miljkovic. Phase change material-based thermal energy storage. *Cell Reports Physical Science*, 2:100540–100540, 08 2021. 4

[50] Eszter Hajba-Horváth, Bence Németh, László Trif, Zoltán May, Miklós Jakab, Andrea Fodor-Kardos, and Tivadar Feczkó. Low temperature energy storage by bio-originated calcium alginate-octyl laurate microcapsules. *Journal of Thermal Analysis and Calorimetry*, 147:13151–13160, 12 2022. 5

[51] Samantha L. Piper, Mega Kar, Douglas R. MacFarlane, Karolina Matuszek, and Jennifer M. Pringle. Ionic liquids for renewable thermal energy storage – a perspective. *Green Chemistry*, 24:102–117, 1 2022. 5

[52] Maria C.M. Sequeira, Bernardo A. Nogueira, Fernando J.P. Caetano, Hermínio P. Diogo, João M.N.A. Fareleira, and Rui Fausto. Di-alkyl adipates as new phase change material for low temperature energy storage. *International Journal of Thermophysics*, 44, 11 2023. 5

[53] Vennapusa Jagadeeswara Reddy, Mohd Fairusham Ghazali, and Sudhakar Kumarasamy. Innovations in phase change materials for diverse industrial applications: A comprehensive review, 6 2024. 5

[54] Jintao Huang, Mengman Weng, Jingfang Yu, Luyi Sun, Hongbo Zeng, Yidong Liu, Wei Zeng, Yonggang Min, and Zhanhu Guo. Advances and applications of phase change materials (pcms) and pcms-based technologies. *ES Materials and Manufacturing*, 13:23–39, 9 2021. 5, 6, 7, 8

[55] Le Zhao, Qiongfen Yu, Ming Li, Yunfeng Wang, Guoliang Li, Shengnan Sun, Jie Fan, and Yali Liu. A review of the innovative application of phase change materials to cold-chain logistics for agricultural product storage, 11 2022. 5

[56] Shilei Zhu, Mai Thanh Nguyen, and Tetsu Yonezawa. Micro- and nano-encapsulated metal and alloy-based phase-change materials for thermal energy storage, 8 2021. 5, 6

[57] Zakir Khan, Zulfiqar Khan, and Abdul Ghafoor. A review of performance enhancement of pcm based latent heat storage system within the context of materials, thermal stability and compatibility. Technical report, 5 2016. 5, 6

[58] Xinghui Zhang, Qili Shi, Lingai Luo, Yilin Fan, Qian Wang, and Guanguan Jia. Research progress on the phase change materials for cold thermal energy storage, 12 2021. 5, 6

[59] Marie Duquesne, Clément Mailhé, Stefania Doppiu, Jean Luc Dauvergne, Sergio Santos-Moreno, Alexandre Godin, Guillaume Fleury, Fabien Rouault, and Elena Palomo Del Barrio. Characterization of fatty acids as biobased organic materials for latent heat storage. *Materials*, 14, 8 2021. 5

[60] Victor M. Nazarychev, Artyom D. Glova, Sergey V. Larin, Alexey V. Lyulin, Sergey V. Lyulin, and Andrey A. Gurtovenko. Cooling-rate computer simulations for the description of crystallization of organic phase-change materials. *International Journal of Molecular Sciences*, 23, 12 2022. 5

[61] Tushar Kanti Maiti, Prakhar Dixit, Amit Suhag, Sakchi Bhushan, Aparna Yadav, Namita Talapatra, and Sujay Chattopadhyay. Advancements in organic and inorganic shell materials for the preparation of microencapsulated phase change materials for thermal energy storage applications, 4 2023. 6, 7

[62] Qi Zhang, Yinlei Li, Jun Song, Xue Ling Zhang, Xuehong Wu, Chongyang Liu, and Yanfang Li. Study on preparation and thermal properties of new inorganic eutectic binary composite phase change materials. *RSC Advances*, 13:16837–16849, 6 2023. 6, 9

[63] Prakhar Dixit, Apoorv Balwani, Tridib Ambardar, Vennapusa Jagadeeswara Reddy, Tushar Kanti Maiti, Adarsh Kumar Pandey, Aravind Dasari, and Sujay Chattopadhyay. A novel shape-stabilized phase change material with tunable thermal conductivity for cold chain applications. *RSC Sustainability*, 1:2305–2318, 10 2023. 6

[64] Amende Sivanathan, Xi Guo, Ziyan Fu, and Mizi Fan. Advances in phase change building materials: An overview, 1 2023. 6

[65] Emiliano Borri, Svetlana Ushak, Yongliang Li, Andrea Frazzica, Yannan Zhang, Yanio E. Milian, Mario Grageda, Dacheng Li, Luisa F. Cabeza, and Vincenza Brancato. Formulation and development of composite materials for thermally driven and storage-integrated cooling technologies: a review, 12 2024. 6, 7, 8

[66] Anas Islam, A. K. Pandey, R. Saidur, Belqasem Aljafari, and V. V. Tyagi. Advancements in foam-based phase change materials: Unveiling leakage control, enhanced thermal conductivity, and promising applications, 12 2023. 6

[67] Otu Okogeri and Vassilis N. Stathopoulos. What about greener phase change materials? a review on biobased phase change materials for thermal energy storage applications, 5 2021. 6

[68] Harald Mehling. Review of classification of pcms, with a focus on the search for new, suitable pcm candidates, 9 2024. 6

[69] Law Torres Sevilla and Jovana Radulovic. Effectiveness of thermal properties in thermal energy storage modeling. *Frontiers in Mechanical Engineering*, 7, 5 2021. 6

[70] Changying Zhao, Jun Yan, Xikun Tian, Xinjie Xue, and Yao Zhao. Progress in thermal energy storage technologies for achieving carbon neutrality, 12 2023. 6, 7

[71] Nicola Bianco, Andrea Fragnito, Marcello Iasiello, Gerardo Maria Mauro, and Luigi Mongibello. Subcooling effect on pcm solidification: A thermostat-like approach to thermal energy storage. *Energies*, 16, 6 2023. 7

[72] Muhammad Imran Khan, Faisal Asfand, and Sami G. Al-Ghamdi. Progress in research and development of phase change materials for thermal energy storage in concentrated solar power. *Applied Thermal Engineering*, 219, 1 2023. 7, 8, 9

[73] Harald Mehling, Jan Leys, Christ Glorieux, and Jan Thoen. Potential new reference materials for caloric measurements on pcm. *SN Applied Sciences*, 3, 2 2021. 8

[74] Sameh A. Nada, Walid G. Alshaer, and Ramy M. Saleh. Segregation/cycling effects on thermophysical properties of salt hydrate phase change materials. *Energy Storage*, 3, 12 2021. 8

[75] Petr Jančík, Michal Schmirler, Tomáš Hyhlík, Adam Bláha, Pavel Sláma, Jakub Devera, and Jan Kouba. Experimental investigation and modelling of a laboratory-scale latent heat storage with cylindrical pcm capsules. *Scientific Reports*, 11, 12 2021. 8

[76] Arnold Martínez, Mauricio Carmona, Cristóbal Cortés, and Inmaculada Arauzo. Experimentally based testing of the enthalpy-porosity method for the numerical simulation of phase change of paraffin-type pcms. *Journal of Energy Storage*, 69:107876, 2023. 8

[77] Adeel Arshad, Mohammed Ibrahim Alabdullatif, Mark Jabbal, and Yuying Yan. Towards the thermal management of electronic devices: A parametric investigation of finned heat sink filled with pcm. *International Communications in Heat and Mass Transfer*, 129, 12 2021. 8

[78] Yaoge Jing, Zhengchuang Zhao, Xiaoling Cao, Qinrong Sun, Yanping Yuan, and Tingxian Li. Ultra-flexible, cost-effective and scalable polymer-based phase change composites via chemical cross-linking for wearable thermal management. *Nature Communications*, 14, 12 2023. 8

[79] Silvia Barbi, Francesco Barbieri, Simona Marinelli, Bianca Rimini, Sebastiano Merchiori, Barbara Larwa, Michele Bottarelli, and Monia Montorsi. Phase change material-sand mixtures for distributed latent heat thermal energy storage: Interaction and performance analysis. *Renewable Energy*, 169:1066–1076, 2021. 8

[80] Allan T. Muzhanje and Hamdy Hassan. Heat transfer characteristics of charging and discharging encapsulated pcms (sp24, sp26 & sp29) for free cooling: impact of geometry and nanomaterials addition. *Journal of Thermal Analysis and Calorimetry*, 148:9919–9936, 10 2023. 8

[81] Ilia Shojaeinasab Chatroudi, Meysam Atashafrooz, Hayder I. Mohammed, Azher M. Abed, and Pouyan Talebizadehsardari. Heat transfer enhancement and free convection assessment in a double-tube latent heat storage unit equipped with optimally spaced circular fins: Evaluation of the melting process. *Frontiers in Energy Research*, 11, 1 2023. 8, 9, 10

[82] Waseem Aftab, Ali Usman, Jinming Shi, Kunjie Yuan, Mulin Qin, and Ruqiang Zou. Phase change material-integrated latent heat storage systems for sustainable energy solutions, 8 2021. 9

[83] Martin Osei, Owen Staveland, Sean McGowan, Justin Brett Unger, Nathan Robert Christler, Matthew Weeman, Marcus Edward Strutz, Matthew Walker, Megan Belle Maun, Nicolas C. Dunning, Marcorios M. Bekheit, Jon Christian Papa Abraham, Liam Cox, Grace Gius, Olivia Hansel, Emmanuel Osei Amoafo, Nichole Hugo, and Pete Schwartz. Phase change thermal storage: Cooking with more power and versatility. *Solar Energy*, 220:1065–1073, 5 2021. 9

[84] Varad Vichare, Anita Nene, and Ashish Utage. Performance analysis of solar immersion heater with phase change material. *Energy Storage*, 6, 2 2024. 9

[85] Karrar A. Hammoodi, Walaa Nasser Abbas, Ali Habeeb Askar, Mohammed Azeez Alomari, Ahmed M. Hassan, Hasan Qahtan Hussein, Abbas Fadhil Khalaf, Mujtaba A. Flayyih, and Saif Ali Kadhim. Cfd simulation of air layer effects on rt42 pcm melting in a square cell. *Scientific Reports*, 15, 2025. 9, 10

[86] Morteza Bayareh and Zahra Ghorbani Kharaji. Comprehensive insights into machine learning and cfd approaches for latent heat energy storage systems, 9 2025. 9

[87] Nguyen Van Hap, Phan Thanh Nhan, and Nguyen Minh Phu. Numerical and experimental investigation of the solar air heater with latent heat storage and fin. *Scientific Reports*, 15:29921, 2025. 10

[88] H. Nemati and Roozbeh Naemi. Phase change material-enhanced shoe sole for foot thermal regulation to prevent hyperthermia. *Thermal Science and Engineering Progress*, 45:102151, 2023. 10

[89] Billy-Joe Bobach, Romain Boman, Diego Celentano, Vincent E. Terrapon, and Jean-Philippe Ponthot. Simulation of the marangoni effect and phase change using the particle finite element method. *Applied Sciences*, 11(24), 2021. 10

[90] Maxence Claeskens, Dorian Bogucki, Simon Février, Martin Lacroix, Romain Boman, Jean-Philippe Ponthot, and Eduardo Fernández. Thermo-fluid simulation of latent heat thermal energy storage devices using the particle finite element method. *International Journal of Numerical Methods for Heat Fluid Flow*, 36(7):2600–2627, 03 2026. 10

[91] Sabine Moench and Robert Dittrich. Influence of natural convection and volume change on numerical simulation of phase change materials for latent heat storage. *Energies*, 15(8), 2022. 10

[92] Daili Feng, Jianfu Nan, Yanhui Feng, Xinxin Zhang, and Yuying Yan. Numerical investigation on improving the heat storage and transfer performance of ceramic /d-mannitol composite phase change materials by bionic graded pores and nanoparticle additives. *International Journal of Heat and Mass Transfer*, 179:121748, 2021. 10

[93] Rahul Joshi, Basant Singh Sikarwar, and Pushpendra Kumar Singh Rathore. Dual phase change material segmentation and orientation effects in shell-and-tube latent heat storage: A validated cfd simulation. *Energy Technology*, 14(1):e202501266, 2026. 10

[94] Simon Bawakyillenuo, Innocent S.K. Agbelie, Aba O. Crentsil, and Stephanie K. Danquah. Preferences of future cooking fuel types among urban and peri-urban households in greater accra region of ghana: Business-as-usual or sustainable pathways? *Energy Policy*, 199, 4 2025. 10

[95] Jerzy Wołoszyn and Krystian Szopa. Shell shape influence on latent heat thermal energy storage performance during melting and solidification. *Energies*, 16(23), 2023. 10

[96] Abbas Fadhil Khalaf, Farhan Lafta Rashid, Mudhar A. Al-Obaidi, Arman Ameen, and Hayder I. Mohammed. Numerical investigation of the effect of an air layer on the melting process of phase change materials. *Materials for Renewable and Sustainable Energy*, 13:291–305, 2024. 10

[97] S. Rahmanian, H. Rahmanian-Koushkaki, M. Moein-Jahromi, and R. Saidur. A novel method to improve the performance of pcm thermal energy storage units using a small oscillator plate-numerical analysis. *Journal of Energy Storage*, 73:108900, 2023. 10

[98] Jerome Droniou, Mohamed Laaziri, and Roland Masson. Discretisations of mixed-dimensional thermo-hydro-mechanical models preserving energy estimates. 2024. 10

[99] Nidhal Ben Khedher, Maryam Ghodrat, Mikhail Sheremet, Amira M. Hussin, Mohamed Houcine Dhaou, S.A.M. Mehryan, and Mohsen Sharifpur. The influence of aspect ratios of two elliptical cylinders on the solid-liquid phase change flow. *Alexandria Engineering Journal*, 86:346–359, 2024. 10

[100] João Pássaro, A. Rebola, Luis Coelho, and J. Conde. Numeric study of geothermal borehole heat exchanger enhancement via phase change material macro encapsulation. *International Journal of Thermofluids*, 16:100245, 11 2022. 10

[101] Wei Biao Ye and Müslüm Arıcı. Exploring mushy zone constant in enthalpy-porosity methodology for accurate modeling convection-diffusion solid-liquid phase change of calcium chloride hexahydrate. *International Communications in Heat and Mass Transfer*, 152, 3 2024. 10

[102] S. R. Hosseini, M. Moghimi, and N. M. Nouri. On the role of surface morphology in impacting-freezing dynamics of supercooled droplets. *Scientific Reports*, 14:12585, 2024. 10

[103] Bouke Johannes Kaaks, Martin Rohde, Jan-Leen Kloosterman, and Danny Lathouwers. An energy-conservative dg-fem approach for solid–liquid phase change. *Numerical Heat Transfer, Part B: Fundamentals*, 84(5):487–513, 2023. 10

[104] Fabrizia Giordano, Adam Buruzs, Manuel Schieder, Maité Goderis, Wim Beyne, Michel De Paepe, and Tilman Barz. Statistical analysis of heat transfer with non-isothermal melting in 116 commercial pcms using the apparent heat capacity method in ansys fluent. *Journal of Energy Storage*, 140:118793, 2025. 13, 14, 32

[105] Rejane De Césaro Oliveski, Fábio Becker, Luiz Alberto Oliveira Rocha, Cesare Biserni, and Gabriel Eduardo Strohm Eberhardt. Design of fin structures for phase change material (pcm) melting process in rectangular cavities. *Journal of Energy Storage*, 35:102337, 2021. 14

[106] Jianping Du, Binjian Nie, Yanping Zhang, Zheng Du, li Wang, and Yulong Ding. Cooling performance of a thermal energy storage-based portable box for cold chain applications. *Journal of Energy Storage*, 28, 4 2020. 18

[107] Technical report. 23, 24, 26

[108] Rasha Abdulrazzak Jasim, Wajdi Qasim Hussen, Mahir Faris Abdulla, Isam Jabbar Ibrahim, and Rozli Zulkifli. Simulation of heat transfer during paraffin and gallium melting and solidification processes utilizing star ccm+. *CFD Letters*, 16:37–54, 3 2024. 32